Transverse Single-Spin Asymmetries and the Universal Nature of Transversity PDFs and Nucleon Tensor Charges

Daniel Pitonyak
Lebanon Valley College, Annville, PA, USA

QCD Evolution Workshop
Pavia, Italy
May 30, 2024

$$S_T^i\, \boldsymbol{h_1^q(x)} = \frac{1}{2}\int \frac{d\xi^-}{2\pi} e^{ixP^+\xi^-}\,\mathrm{Tr}[\langle P,S|\bar{\psi}_q(0)\mathcal{W}(0,\xi^-)\psi_q(\xi^-)i\sigma^{i+}\gamma_5|P,S\rangle]$$

transversity PDF - universal parton density that quantifies the degree of transverse polarization of quarks within a transversely polarized nucleon

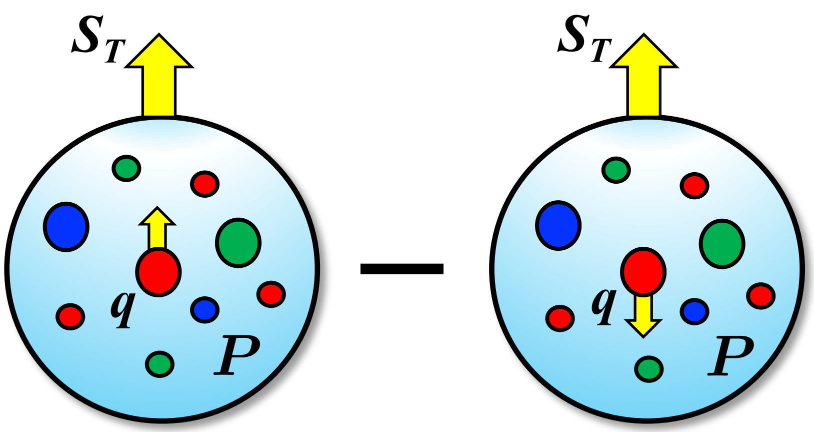

$$\boldsymbol{\delta q} \equiv \int_0^1 dx\,[h_1^q(x) - h_1^{\bar{q}}(x)]$$

tensor charge for an individual flavor

$$\boldsymbol{g_T} \equiv \delta u - \delta d$$

isovector combination

Anselmino, et al. (2007, 2009, 2013, 2015);
Goldstein, et al. (2014); Kang, et al. (2016); Radici, et al. (2013, 2015, 2018);
Benel, et al. (2020); D'Alesio, et al. (2020); Cammarota, et al. (2020);
Gamberg, et al. (2022); Cocuzza, et al. (2024)

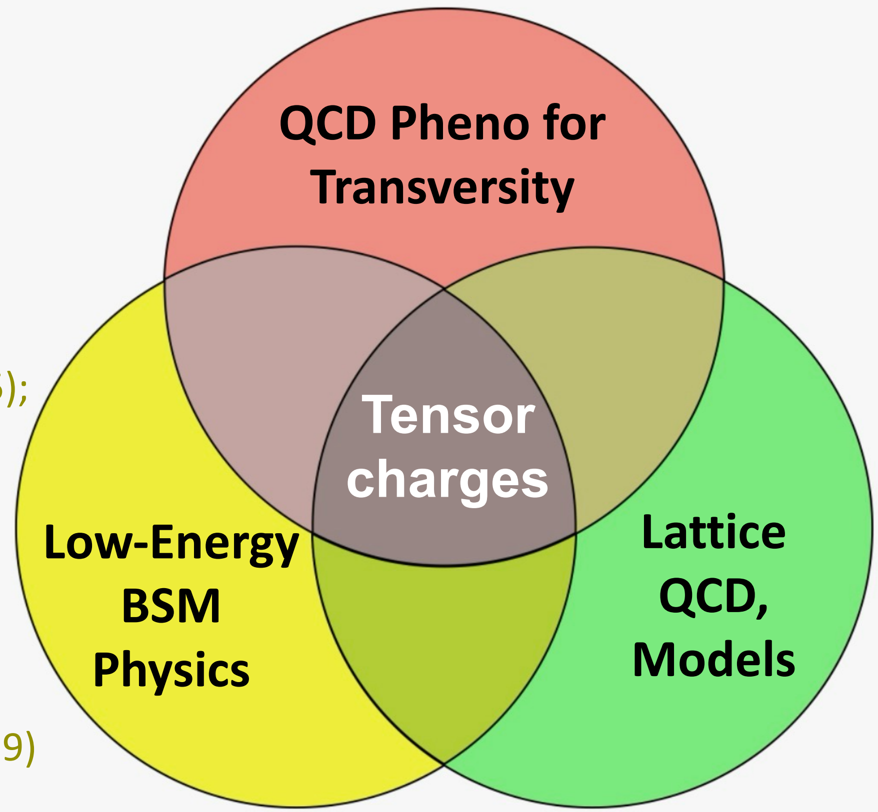

Herczeg (2001);
Erler, Ramsey-Musolf (2005);
Pospelov, Ritz (2005);
Severijns, et al. (2006);
Cirigliano, et al. (2013);
Courtoy, et al. (2015);
Yamanaka, et al. (2017);
Liu, et al. (2018);
Gonzalez-Alonso, et al. (2019)

He, Ji (1995);
Barone, et al. (1997);
Schweitzer, et al. (2001);
Gamberg, Goldstein (2001);
Pasquini, et al. (2005);
Wakamatsu (2007);
Lorce (2009);
Gupta, et al. (2018);
Yamanaka, et al. (2018);
Hasan, et al. (2019);
Alexandrou, et al. (2019, 2023);
Yamanaka, et al. (2013);
Pitschmann, et al. (2015);
Xu, et al. (2015);
Wang, et al. (2018);
Liu, et al. (2019);
Gao, et al. (2023)

Updated QCD Global Analysis of TSSAs for Single-Hadron Fragmentation

Gamberg, Malda, Miller, DP, Prokudin, Sato, Phys. Rev. D **106**, 034014 (2022)

User-friendly jupyter notebook to calculate functions and asymmetries:
https://colab.research.google.com/github/pitonyak25/jam3d_dev_lib/blob/main/JAM3D_Library.ipynb

LHAPDF tables available (thanks to C. Cocuzza):
https://github.com/pitonyak25/jam3d_dev_lib/tree/main/LHAPDF_tables

Jefferson Lab Angular Momentum Collaboration

$\ell p^{\uparrow} \to \ell h X$

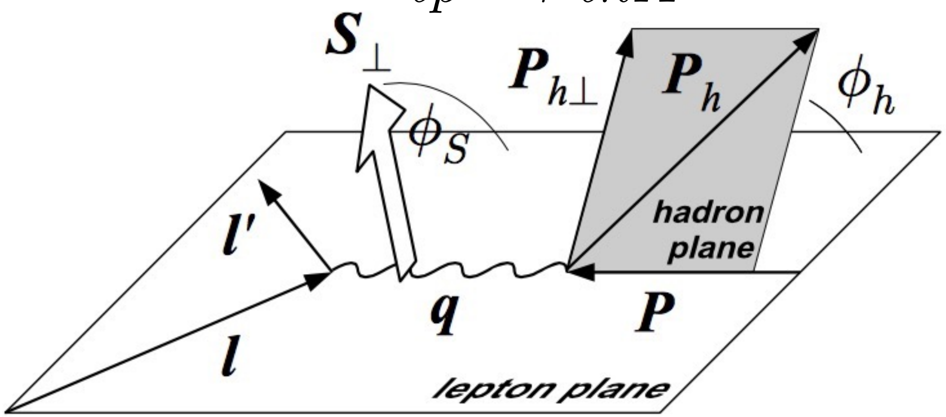

$\{\pi, p\} p^{\uparrow} \to \{\ell^+\ell^-, W^{\pm}, Z\} X$

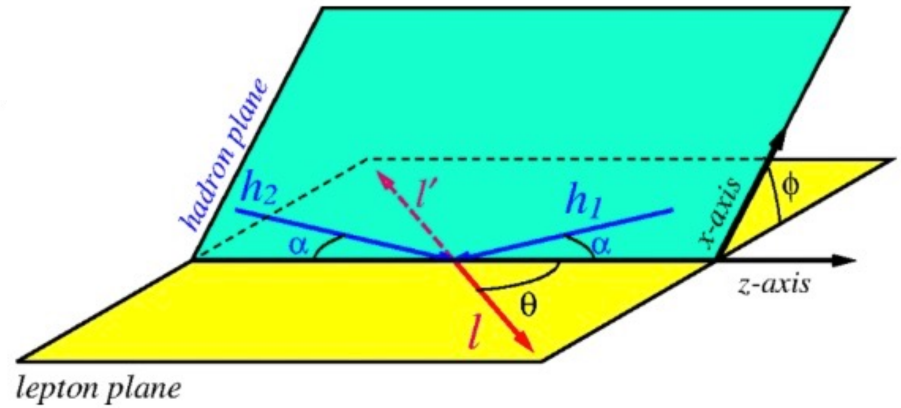

$$F_{UT}^{\sin(\phi_h - \phi_S)} = \mathcal{C}\left[-\frac{\hat{h}\cdot\vec{k}_T}{M} \boldsymbol{f_{1T}^{\perp}} D_1\right]$$

$$F_{TU}^{\sin\phi} = \mathcal{C}\left[-\frac{\hat{h}\cdot\vec{k}_{aT}}{M_a} \boldsymbol{f_{1T}^{\perp}}\, \bar{f}_1\right]$$

TMD/Collins-Soper-Sterman (CSS) Evolution

OPE

Sudakov exponentials (gluon radiation)

$$\tilde{f}_{1T}^{\perp(1)}(x, b_T; Q^2, \mu_Q) \sim F_{FT}(x, x; \mu_{b_*}) \exp\left[-S_{pert}(b_*(b_T); \mu_{b_*}, Q, \mu_Q) - S_{NP}^{f_{1T}^{\perp}}(b_T, Q)\right]$$

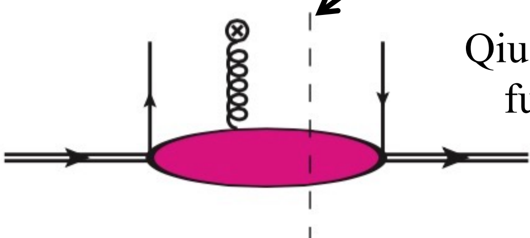

Qiu-Sterman function

$$g_{f_{1T}^{\perp}}(x, b_T) + g_K(b_T)\ln(Q/Q_0)$$

(Aybat, et al. (2012); Bury, et al. (2021); Echevarria, et al. (2014, 2021))

Parton model

$$\pi F_{FT}(x,x) = \int d^2\vec{k}_T\, \frac{k_T^2}{2M^2} f_{1T}^{\perp}(x, k_T^2) \equiv f_{1T}^{\perp(1)}(x)$$

(Boer, Mulders, Pijlman (2003), see also del Rio, et al. (2024))

$$\ell N^\uparrow \to \ell h X \qquad\qquad e^+e^- \to h_1 h_2 X$$

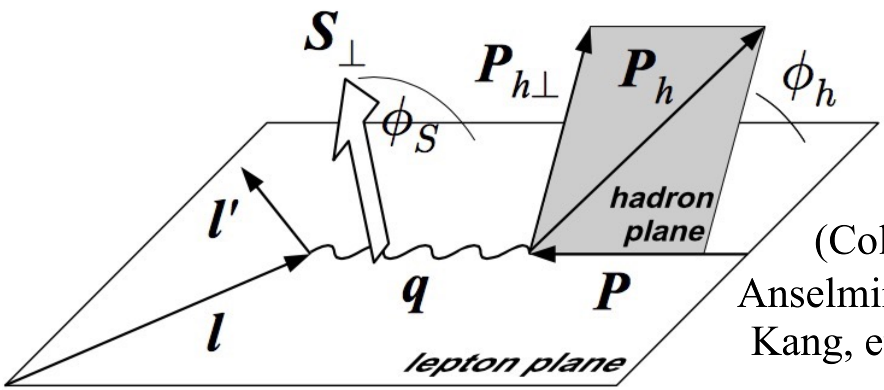

(Collins (1992); Anselmino, et al. (2007); Kang, et al. (2016); …)

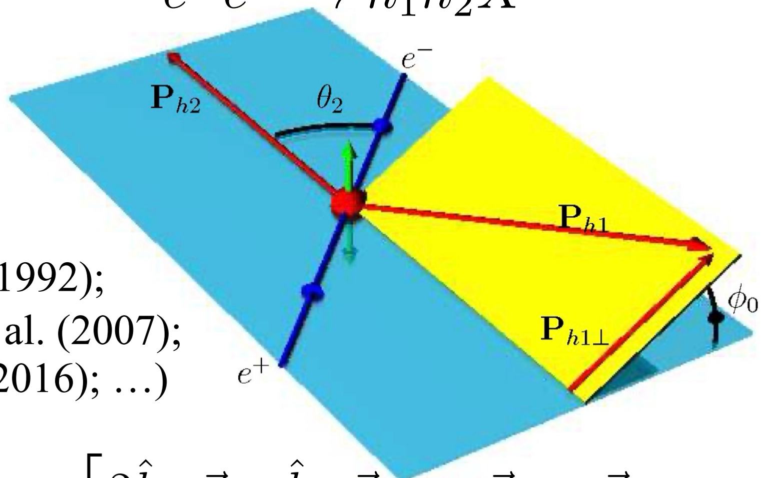

$$F_{UT}^{\sin(\phi_h+\phi_S)} = \mathcal{C}\left[-\frac{\hat{h}\cdot\vec{p}_\perp}{M_h}\boldsymbol{h_1 H_1^\perp}\right] \qquad F_{UU}^{\cos(2\phi_0)} = \mathcal{C}\left[\frac{2\hat{h}\cdot\vec{p}_{a\perp}\,\hat{h}\cdot\vec{p}_{b\perp} - \vec{p}_{a\perp}\cdot\vec{p}_{b\perp}}{M_a M_b}\boldsymbol{H_1^\perp \bar{H}_1^\perp}\right]$$

TMD/Collins-Soper-Sterman (CSS) Evolution

OPE — Sudakov exponentials (gluon radiation)

$$\boldsymbol{\tilde{h}_1(x, b_T; Q^2, \mu_Q)} \sim \boldsymbol{h_1(x;\mu_{b_*})}\exp\left[-S_{pert}(b_*(b_T);\mu_{b_*},Q,\mu_Q) - S_{NP}^{h_1}(b_T,Q)\right]$$

$$\boldsymbol{\tilde{H}_1^{\perp(1)}(z, b_T; Q^2, \mu_Q)} \sim \boldsymbol{H_1^{\perp(1)}(z;\mu_{b_*})}\exp\left[-S_{pert}(b_*(b_T);\mu_{b_*},Q,\mu_Q) - S_{NP}^{H_1^\perp}(b_T,Q)\right]$$

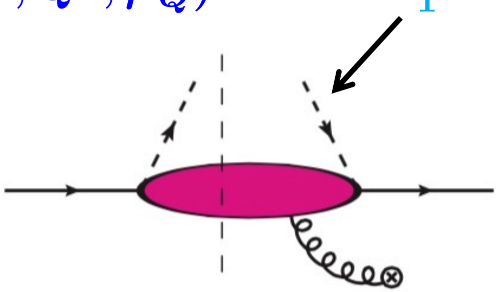

qgq fragmentation function

Parton model

$$h_1(x) = \int d^2\vec{k}_T\, h_1(x,\vec{k}_T^2)$$

$$H_1^{\perp(1)}(z) = z^2\int d^2\vec{p}_\perp \frac{p_\perp^2}{2M_h^2} H_1^\perp(z, z^2 p_\perp^2)$$

$p^{\uparrow}p \to hX$

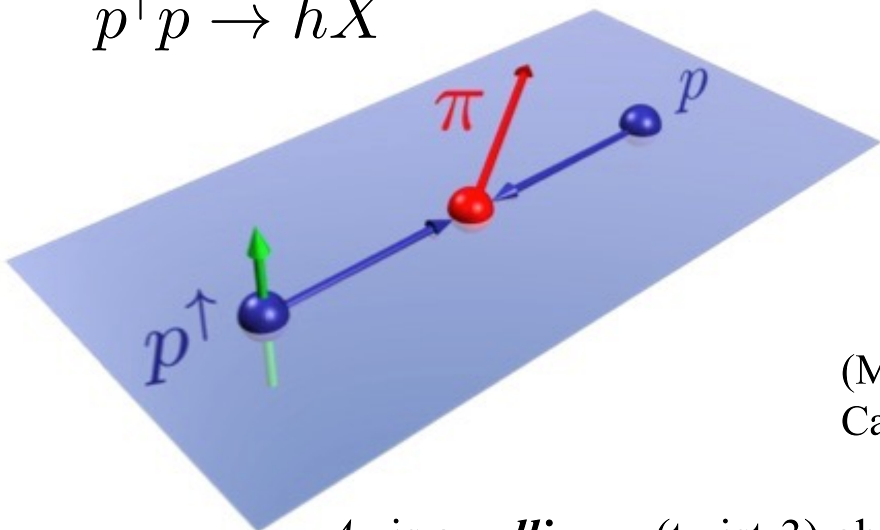

$$d\Delta\sigma(S_T) \sim \underbrace{H_{QS} \otimes f_1 \otimes \boldsymbol{F_{FT}} \otimes D_1}_{\text{Qiu-Sterman term}}$$

$$+ \underbrace{H_F \otimes f_1 \otimes \boldsymbol{h_1} \otimes \left(\boldsymbol{H_1^{\perp(1)}}, \boldsymbol{\tilde{H}}\right)}_{\text{Fragmentation term}}$$

(Metz, DP (2012); Kanazawa, et al. (2014); Cammarota, et al. (2020); Gamberg, et al. (2017, 2022))

A_N is a ***collinear*** (twist-3) observable

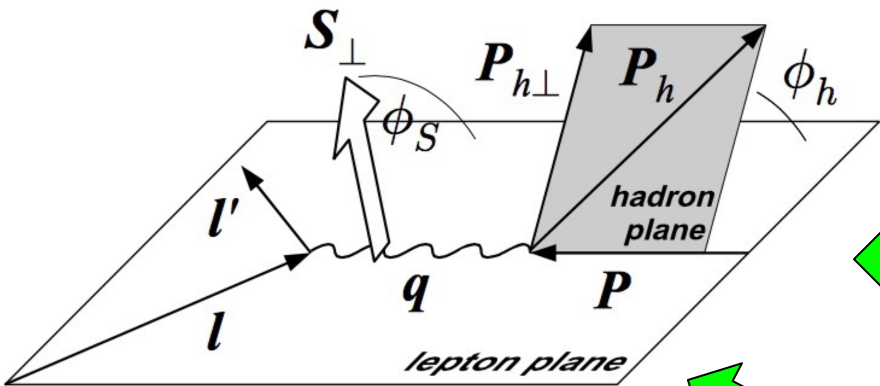

$h_1, \ F_{FT}, \ H_1^{\perp(1)}, \ \tilde{H}$

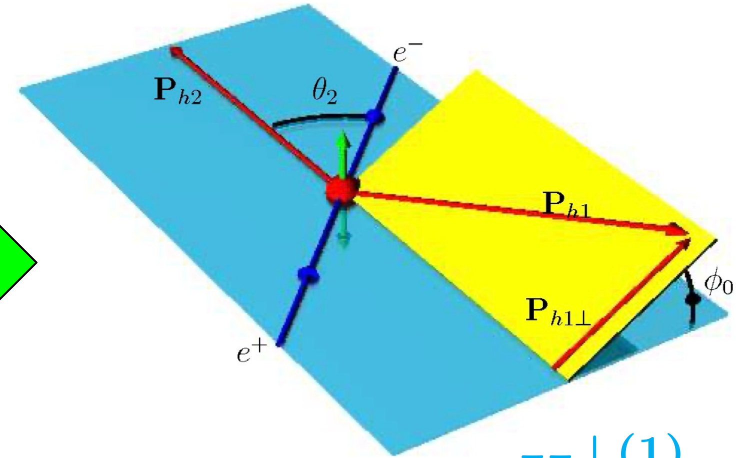

$H_1^{\perp(1)}$

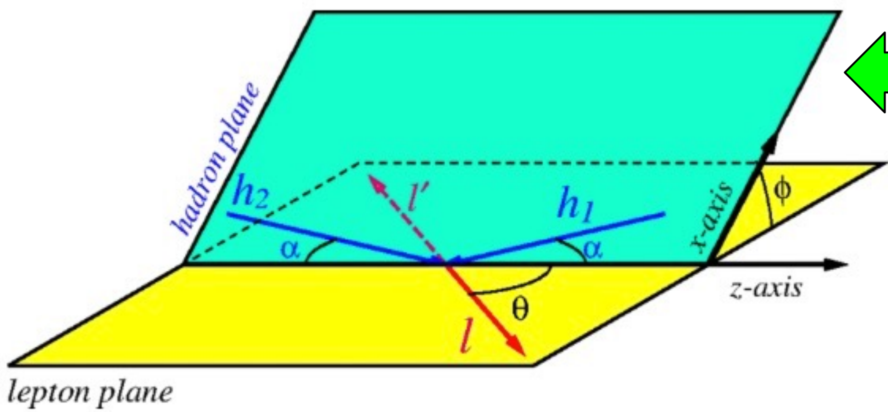

F_{FT}

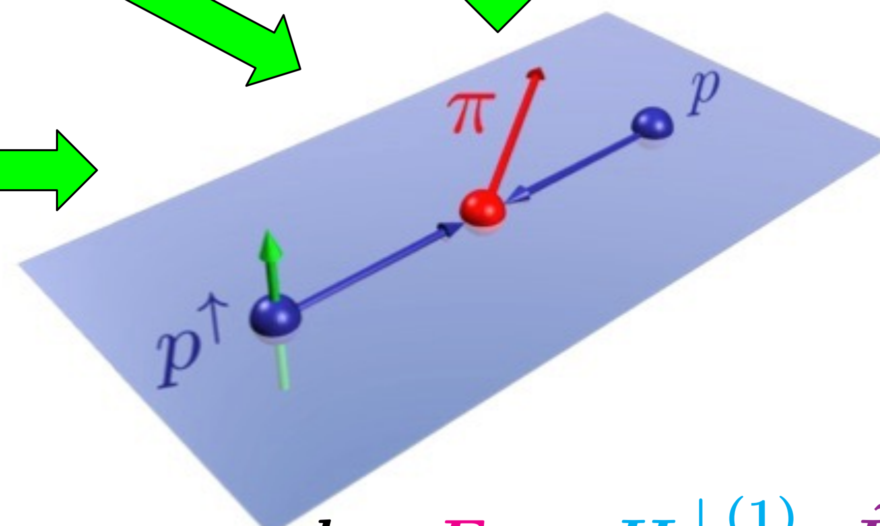

$h_1, \ F_{FT}, \ H_1^{\perp(1)}, \ \tilde{H}$

- Analyze TSSAs in SIDIS, Drell-Yan, e^+e^- annihilation, and proton-proton collisions and extract

$$\boldsymbol{h_1(x),\ F_{FT}(x,x),\ H_1^{\perp(1)}(z),\ \tilde{H}(z)}$$

along with the relevant transverse momentum widths for the Sivers, transversity, and Collins functions: $\langle k_T^2\rangle_{f_{1T}^\perp}, \langle k_T^2\rangle_{h_1}, \langle p_\perp^2\rangle_{H_1^\perp}^{fav}, \langle p_\perp^2\rangle_{H_1^\perp}^{unf}$

- We use a Gaussian ansatz: $F^q(x,k_T^2) \sim F^q(x)e^{-k_T^2/\langle k_T^2\rangle}$ where

$$F^q(x) = \frac{N_q\, x^{a_q}(1-x)^{b_q}(1+\gamma_q\, x^{\alpha_q}(1-x)^{\beta_q})}{\mathrm{B}[a_q+2, b_q+1] + \gamma_q \mathrm{B}[a_q+\alpha_q+2, b_q+\beta_q+1]}$$

NB. $\{\gamma, \alpha, \beta\}$ only used for $H_1^{\perp(1)}(x)$, $b_u = b_d$ for $h_1(x), f_{1T}^{\perp(1)}(x)$

- DGLAP-type evolution for the collinear functions analogous to Duke & Owens (1984): double-log Q^2-dependent term explicitly added to the parameters

- Additional data/constraints included in the fit compared to 2020:
  - Collins and Sivers effects (3D-binned) SIDIS data from HERMES (2020)
  - $A_{UT}^{\sin\phi_S}$ data (x and z projections only) from HERMES (2020)

$$\int d^2\vec{P}_{hT}\, F_{UT}^{\sin\phi_S} = -\frac{x}{z}\sum_q e_q^2\, \frac{2M_h}{Q}\, h_1^{q/N}(x)\, \tilde{H}^{h/q}(z)$$

  - Lattice data on g_T at the physical pion mass from ETMC (Alexandrou, et al. (2019))

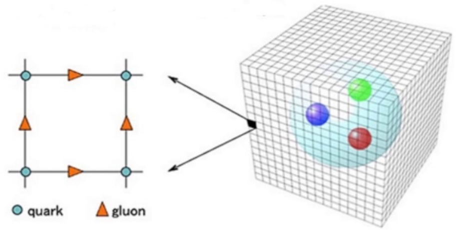

  - Imposing the Soffer bound on transversity: $|h_1^q(x)| \leq \frac{1}{2}(f_1^q(x) + g_1^q(x))$

Generate "data" (central value and 1-σ uncertainty) using recent simultaneous fit of f_1 and g_1 from Cocuzza, et al. (2022) and add to the χ^2 if SB is violated by more than the uncertainty in the data

$$\chi^2/N_{\text{pts.}} = 647/634 = 1.02$$

Observable	Reactions	Non-Perturbative Function(s)	χ^2/npts
$A_{UT}^{\sin(\phi_h-\phi_S)}$	$e+(p,d)^\uparrow \to e+(\pi^+,\pi^-,\pi^0)+X$	$f_{1T}^\perp(x,\vec{k}_T^2)$	$182.9/166 = 1.10$
$A_{UT}^{\sin(\phi_h+\phi_S)}$	$e+(p,d)^\uparrow \to e+(\pi^+,\pi^-,\pi^0)+X$	$h_1(x,\vec{k}_T^2), H_1^\perp(z,z^2\vec{p}_T^2)$	$181.0/166 = 1.09$
$^*A_{UT}^{\sin\phi_S}$	$e+p^\uparrow \to e+(\pi^+,\pi^-,\pi^0)+X$	$h_1(x), \tilde{H}(z)$	$18.6/36 = 0.52$
$A_{UC/UL}$	$e^+ + e^- \to \pi^+\pi^-(UC,UL)+X$	$H_1^\perp(z,z^2\vec{p}_T^2)$	$154.9/176 = 0.88$
$A_{T,\mu^+\mu^-}^{\sin\phi_S}$	$\pi^- + p^\uparrow \to \mu^+\mu^- + X$	$f_{1T}^\perp(x,\vec{k}_T^2)$	$6.92/12 = 0.58$
$A_N^{W/Z}$	$p^\uparrow + p \to (W^+,W^-,Z)+X$	$f_{1T}^\perp(x,\vec{k}_T^2)$	$30.8/17 = 1.81$
A_N^π	$p^\uparrow + p \to (\pi^+,\pi^-,\pi^0)+X$	$h_1(x), F_{FT}(x,x) = \frac{1}{\pi} f_{1T}^{\perp(1)}(x), H_1^{\perp(1)}(z), \tilde{H}(z)$	$70.4/60 = 1.17$
Lattice g_T	——	$h_1(x)$	$1.82/1 = 1.82$

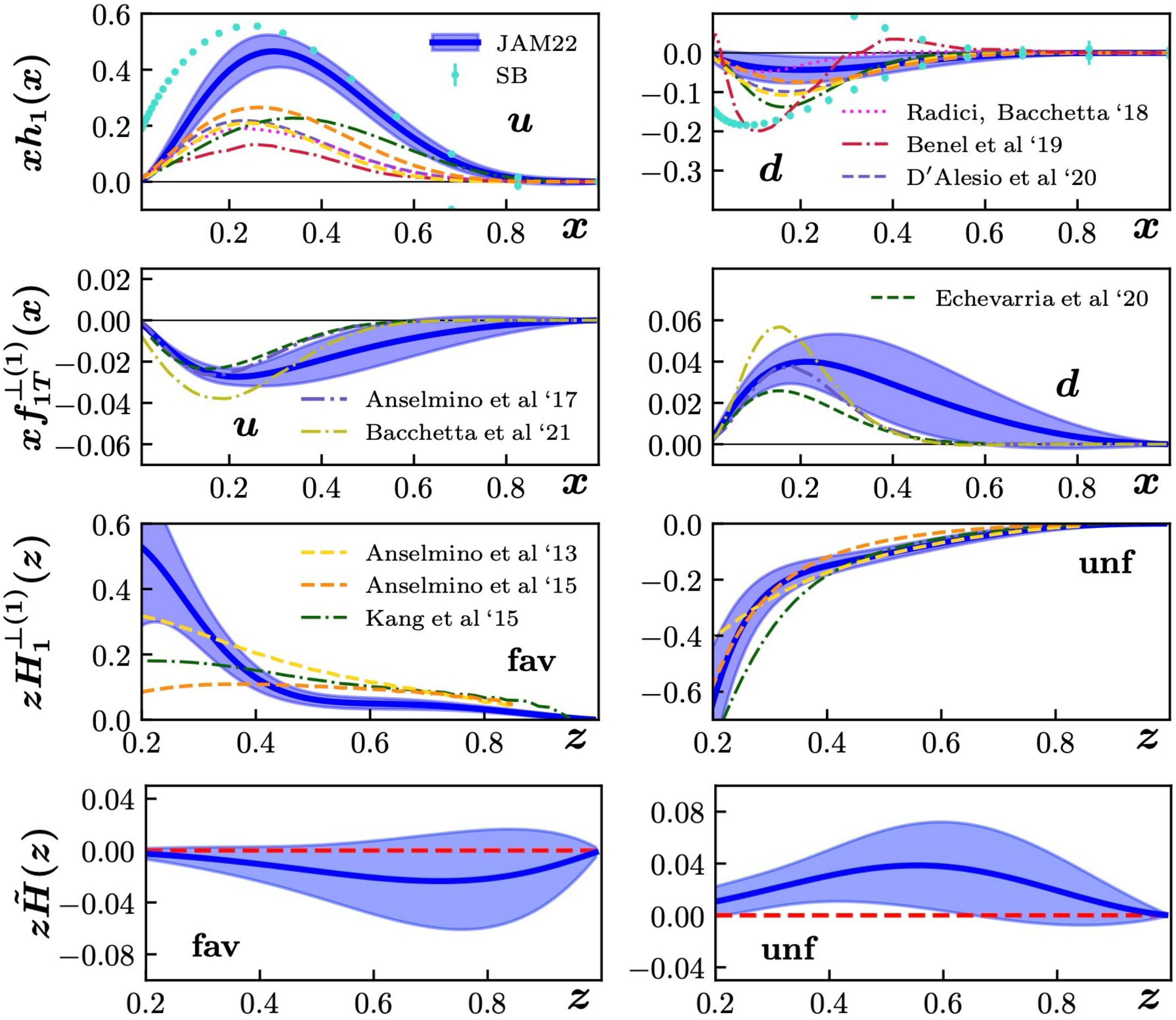

First direct information from experiment on $\tilde{H}(z)$

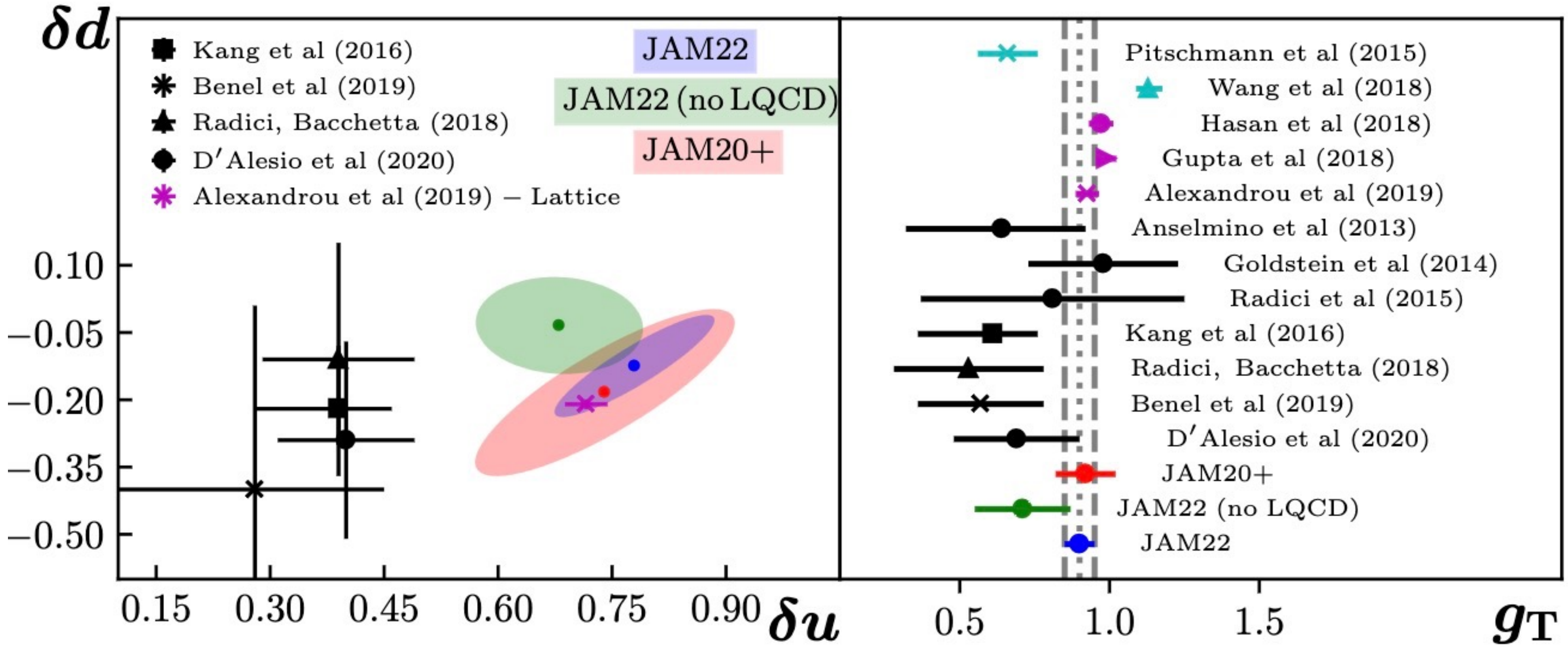

- TMD that only include e^+e^- and SIDIS Collins effect data (e.g., Kang, et al. (2016), D'Alesio, et al. (2020)) and dihadron analyses (e.g., Radici, Bacchetta (2018); Benel, Courtoy, Ferro-Hernandez (2019)), are generally below the lattice values for g_T and δu
- Note that one initially finds JAM3D-22 has more tension with lattice, but this does *not* imply phenomenology and lattice are incompatible – one can only fully answer this by including lattice data in the analysis (use it as a prior)
- **Once g_T is included (as a Bayesian prior), we find the non-perturbative functions can accommodate it *and still describe the experimental data well***

QCD Global Analysis of TSSAs for Dihadron Fragmentation

DP, Cocuzza, Metz, Prokudin, Sato, Phys. Rev. Lett. **132**, 011902 (2024)

Cocuzza, Metz, DP, Prokudin, Sato, Seidl, Phys. Rev. Lett. **132**, 091901 (2024)

Cocuzza, Metz, DP, Prokudin, Sato, Seidl, Phys. Rev. D **109**, 034024 (2024)

User-friendly jupyter notebook to calculate transversity PDFs and DiFFs:
https://colab.research.google.com/github/prokudin/JAMDiFF_library/blob/main/JAMDiFF_Library.ipynb

LHAPDF tables available for transversity PDFs:
https://github.com/prokudin/JAMDiFF_library/tree/main/lhapdf

Jefferson Lab Angular Momentum Collaboration

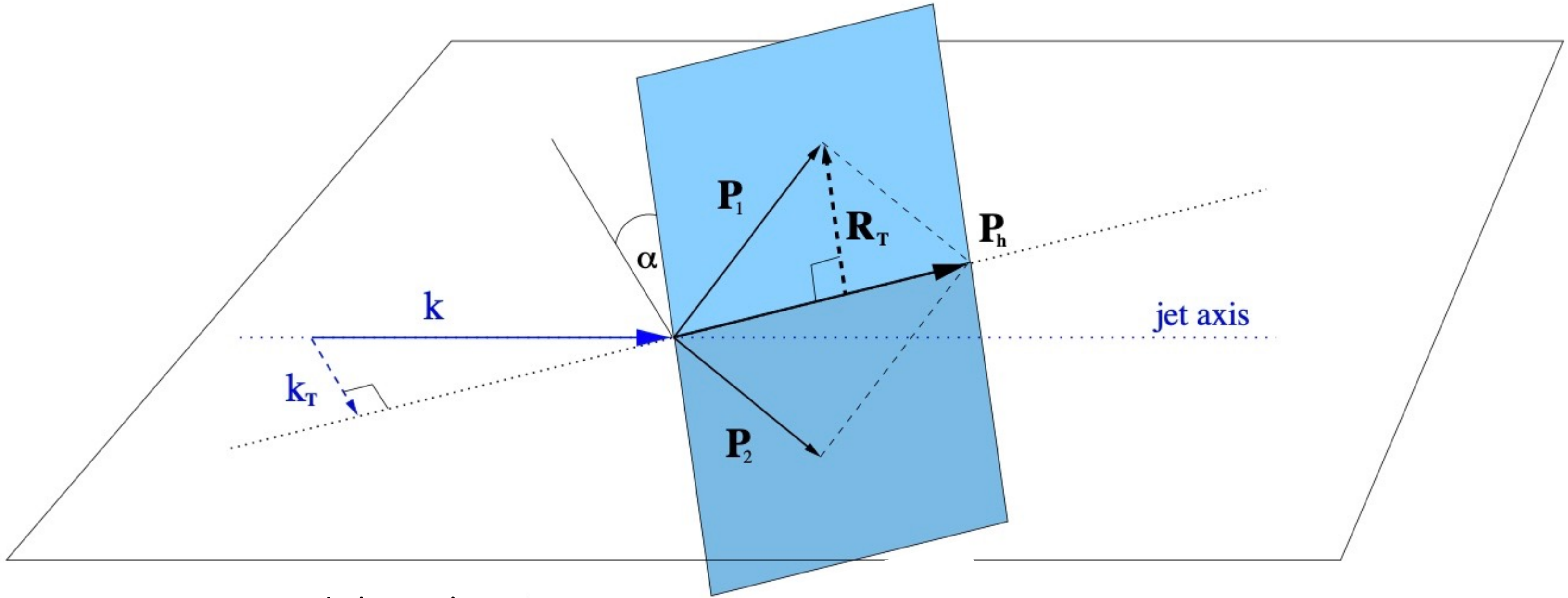

From Bianconi, et al. (2000)

Bianconi, et al. (2000); Bacchetta, Radici (2003, 2004), …

$$P_h = P_1 + P_2 \qquad R = (P_1 - P_2)/2 \qquad z = z_1 + z_2 \qquad \zeta = (z_1 - z_2)/z$$

$$P_1 = \left(\frac{M_1^2 + \vec{R}_T^2}{(1+\zeta)P_h^-}, \frac{1+\zeta}{2}P_h^-, \vec{R}_T \right) \qquad P_2 = \left(\frac{M_2^2 + \vec{R}_T^2}{(1-\zeta)P_h^-}, \frac{1-\zeta}{2}P_h^-, -\vec{R}_T \right)$$

$$\vec{R}_T^2 = \frac{1-\zeta^2}{4}M_h^2 - \frac{1-\zeta}{2}M_1^2 - \frac{1+\zeta}{2}M_2^2$$

$$e^+e^- \to (h_1h_2)(\bar{h}_1\bar{h}_2)\,X \qquad \ell\,N^{\uparrow} \to \ell\,(h_1h_2)\,X \qquad p^{\uparrow}p \to (h_1h_2)\,X$$

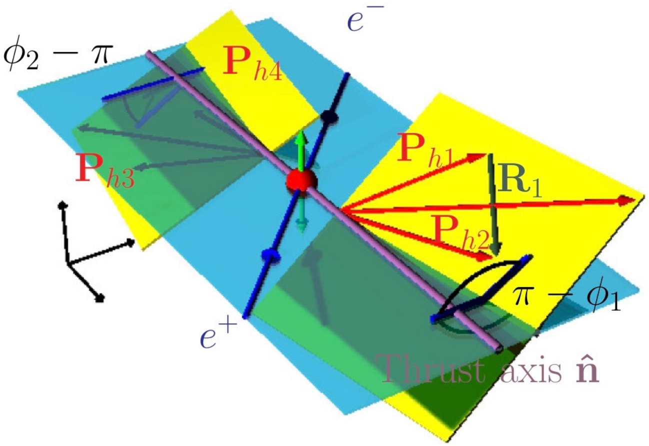

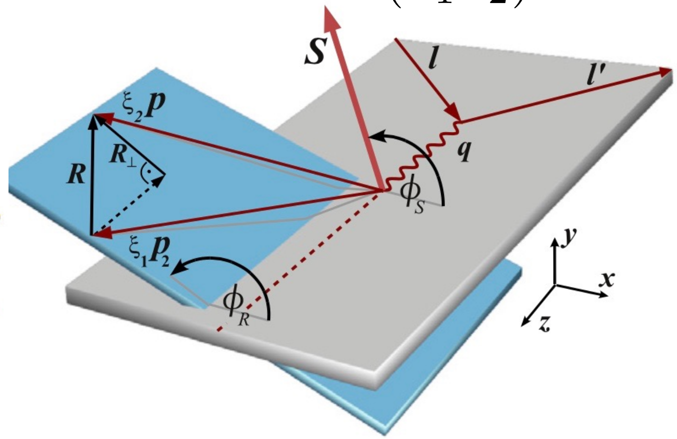

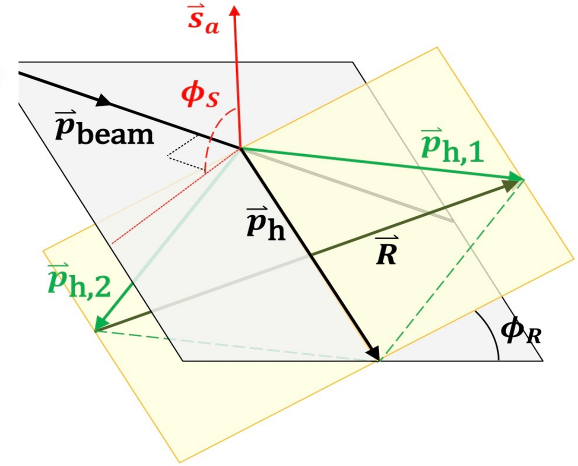

(Collins, et al. (1994); Bianconi, et al. (2000); Bacchetta, Radici (2003, 2004); Courtoy, et al. (2012); Matevosyan, et al. (2018); Radici, et al. (2013, 2015, 2018); Benel, et al. (2020), …)

$$a_{12R} = \frac{\sin^2\theta_2 \sum_q e_q^2\, H_1^{\sphericalangle,q}(z, M_h)\, H_1^{\sphericalangle,\bar{q}}(\bar{z}, \overline{M}_h)}{(1+\cos^2\theta_2)\sum_q e_q^2\, \boldsymbol{D_1^q(z, M_h) D_1^{\bar{q}}(\bar{z}, \overline{M}_h)}}$$

Artru-Collins asymmetry

Note: D_1 can be constrained using data on $d\sigma/dzdM_h$ from BELLE (2017)

$$\frac{d\sigma}{dz\,dM_h} = \frac{4\pi N_c \alpha_{\rm em}^2}{3Q^2}\sum_q e_q^2\, \boldsymbol{D_1^q(z, M_h)}$$

$$A_{UT}^{\sin(\phi_R+\phi_S)} = \frac{\sum_q e_q^2\, \boldsymbol{h_1^q(x)}\, H_1^{\sphericalangle,q}(z, M_h)}{\sum_q e_q^2\, f_1^q(x)\, \boldsymbol{D_1^q(z, M_h)}}$$

$$A_{UT}^{\sin(\phi_R-\phi_S)} \sim \frac{\frac{d\Delta\hat{\sigma}_{a^\uparrow b\to c^\uparrow}}{d\hat{t}} \otimes \boldsymbol{h_1^a(x_a)} \otimes f_1^b(x_b) \otimes H_1^{\sphericalangle,c}(z, M_h)}{\frac{d\hat{\sigma}_{ab\to c}}{d\hat{t}} \otimes f_1^a(x_a) \otimes f_1^b(x_b) \otimes \boldsymbol{D_1^c(z, M_h)}}$$

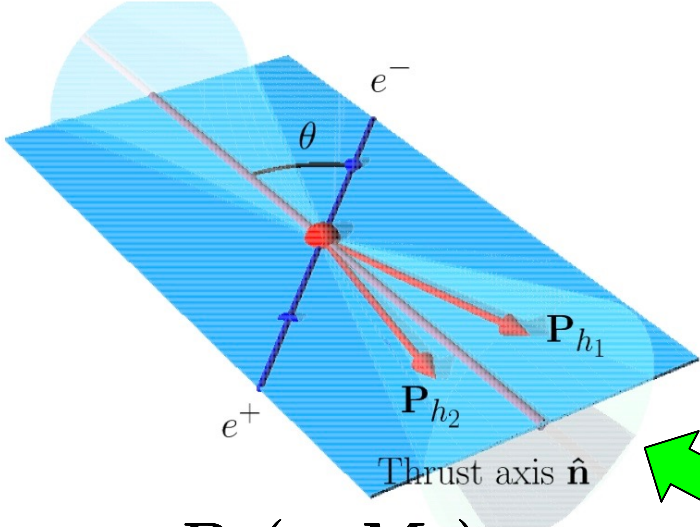

$$D_1(z, M_h)$$

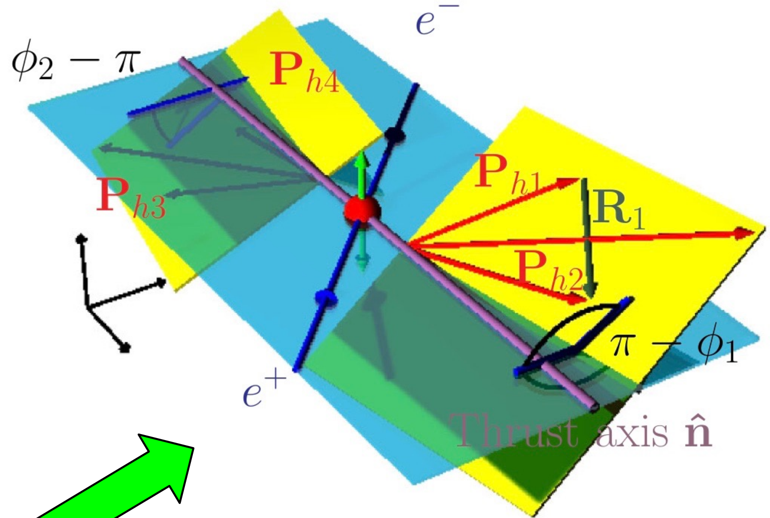

$$H_1^{\sphericalangle}(z, M_h), D_1(z, M_h)$$

DiFFs and transversity PDFs extracted simultaneously

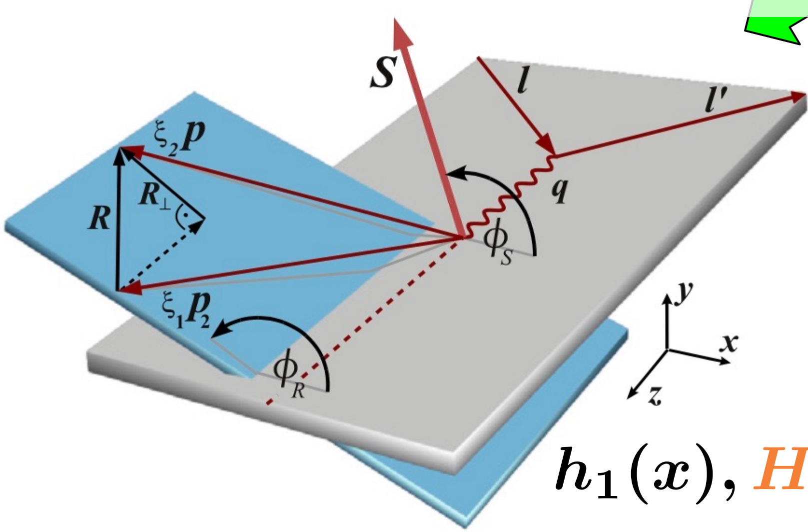

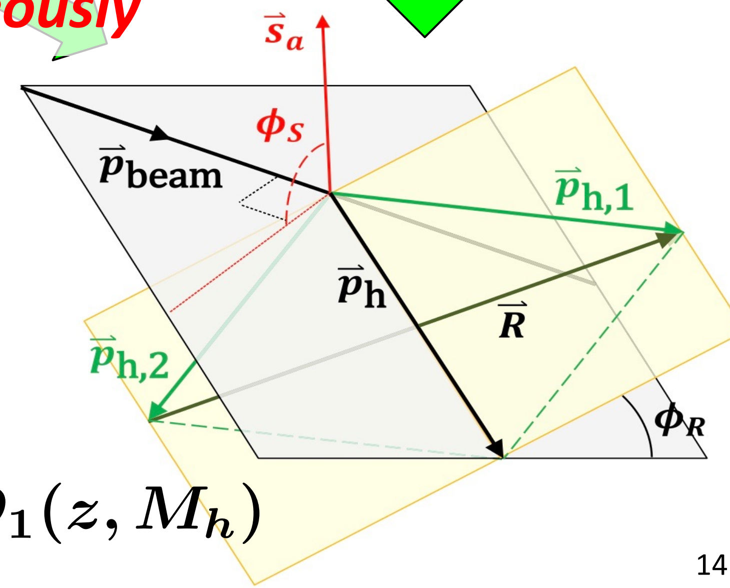

$$h_1(x), H_1^{\sphericalangle}(z, M_h), D_1(z, M_h)$$

- Analyze TSSAs for $\pi^+\pi^-$ production in e^+e^- annihilation, SIDIS, and proton-proton collisions and extract

$$h_1(x),\, H_1^{\sphericalangle}(z, M_h),\, D_1(z, M_h)^*$$

*Also need data from PYTHIA for flavor separation and to constrain the gluon $D_1(z,M_h)$

- We use the following functional form for the transversity PDFs u_v, d_v, and $\bar{u} = -\bar{d}$ (from large-N_c limit (Pobylitsa (2003))) and impose the Soffer bound

$$F(x) \sim N x^{\alpha} (1-x)^{\beta} (1 + \gamma\sqrt{x} + \delta x)$$

Use constraint from small-x asymptotics (Kovchegov, Sievert (2019))

$$\alpha \xrightarrow{x\to 0} 1 - 2\sqrt{\frac{\alpha_s N_c}{2\pi}} \quad \Longrightarrow \quad \alpha = 0.170 \pm 0.085$$

50% uncertainty due to unaccounted for $1/N_c$ and NLO corrections

- Analyze TSSAs for $\pi^+\pi^-$ production in e^+e^- annihilation, SIDIS, and proton-proton collisions and extract

$$\boldsymbol{h_1(x), H_1^{\sphericalangle}(z, M_h), D_1(z, M_h)}^*$$

*Also need data from PYTHIA for flavor separation and to constrain the gluon $D_1(z,M_h)$

- We use the following functional form for the transversity PDFs u_v, d_v, and $\bar{u} = -\bar{d}$ (from large-N_c limit (Pobylitsa (2003))) and impose the Soffer bound

$$F(x) \sim N x^{\alpha} (1-x)^{\beta} (1 + \gamma\sqrt{x} + \delta x)$$

- The DiFFs $D_1(z, M_h), H_1^{\sphericalangle}(z, M_h)$ use the same functional form as above ($x \rightarrow z$) for the z dependence, which is repeated on a grid in M_h (more finely spaced around the resonances) and interpolated to obtain the function value at any M_h

- Perform the analysis with and without LQCD data **as a Bayesian prior** for the tensor charges $\boldsymbol{\delta} u, \boldsymbol{\delta} d$ from ETMC (Alexandrou, et al. (2019)) and PNDME (Gupta, et al. (2018)) (physical pion mass and 2+1+1 flavors)

➢ Remark about χ^2 definition and Bayesian priors

$$\mathcal{P}(\boldsymbol{a}|\text{data}) \propto \mathcal{L}(\boldsymbol{a},\text{data})\,\pi(\boldsymbol{a}) \qquad \mathcal{L}(\boldsymbol{a},\text{data}) = \exp\Big(-\frac{1}{2}\chi^2(\boldsymbol{a},\text{data})\Big)$$

$$\chi^2(\boldsymbol{a}) = \sum_{e,i}\left(\frac{d_{e,i} - \sum_k r_{e,k}\beta^k_{e,i} - T_{e,i}(\boldsymbol{a})/N_e}{\alpha_{e,i}}\right)^2$$

Only experimental data included in the χ^2 function (no LQCD)

$$\pi(\boldsymbol{a}) = \prod_l \Theta\big((a_l - a_l^{\min})(a_l^{\max} - a_l)\big) \prod_f \prod_i \exp\left\{-\frac{1}{2}\left(\frac{d_{f,i} - T_{f,i}(\boldsymbol{a})}{\alpha_{f,i}}\right)^2\right\}$$
$$\times \prod_e \prod_k \exp\left\{-\frac{1}{2}r^2_{e,k}\right\} \prod_e \exp\left\{-\frac{1}{2}\left(\frac{1-N_e}{\delta N_e}\right)^2\right\} \exp\left\{-\frac{1}{2}\Delta^2_{D_1<0}\right\} \exp\left\{-\frac{1}{2}\Delta^2_{|H_1^{\sphericalangle}|>D_1}\right\} \exp\left\{-\frac{1}{2}\Delta^2_{\text{SB}}\right\}$$

LQCD data included as a prior

Experiment	Binning	$N_{\rm dat}$	$\chi^2_{\rm red}$ JAMDiFF (w/ LQCD)	(no LQCD)	(SIDIS only)
Belle (cross section) [64]	z, M_h	1094	1.01	1.01	1.01
Belle (Artru-Collins) [111]	z, M_h	55	1.27	1.24	1.28
	$M_h, \overline{M}_h$	64	0.60	0.60	0.60
	$z, \bar{z}$	64	0.42	0.42	0.41
HERMES [117]	$x_{\rm bj}$	4	1.77	1.70	1.67
	M_h	4	0.41	0.42	0.47
	z	4	1.20	1.17	1.13
COMPASS (p) [116]	$x_{\rm bj}$	9	1.98	0.65	0.59
	M_h	10	0.92	0.94	0.93
	z	7	0.77	0.60	0.63
COMPASS (D) [116]	$x_{\rm bj}$	9	1.37	1.42	1.22
	M_h	10	0.45	0.37	0.38
	z	7	0.50	0.46	0.46
STAR [120] $\sqrt{s} = 200$ GeV $R < 0.3$	$M_h, \eta < 0$	5	2.57	2.56	—
	$M_h, \eta > 0$	5	1.34	1.55	—
	$P_{hT}, \eta < 0$	5	0.98	1.00	—
	$P_{hT}, \eta > 0$	5	1.73	1.74	—
	η	4	0.52	1.46	—
STAR [96] $\sqrt{s} = 500$ GeV $R < 0.7$	$M_h, \eta < 0$	32	1.30	1.10	—
	$M_h, \eta > 0$	32	0.81	0.78	—
	$P_{hT}, \eta > 0$	35	1.09	1.07	—
	η	7	2.97	1.83	—
ETMC δu [77]	—	1	0.71	—	—
ETMC δd [77]	—	1	1.02	—	—
PNDME δu [71]	—	1	8.68	—	—
PNDME δd [71]	—	1	0.04	—	—
Total $\chi^2_{\rm red}$ ($N_{\rm dat}$)			**1.01** (1475)	**0.98** (1471)	0.96 (1341)

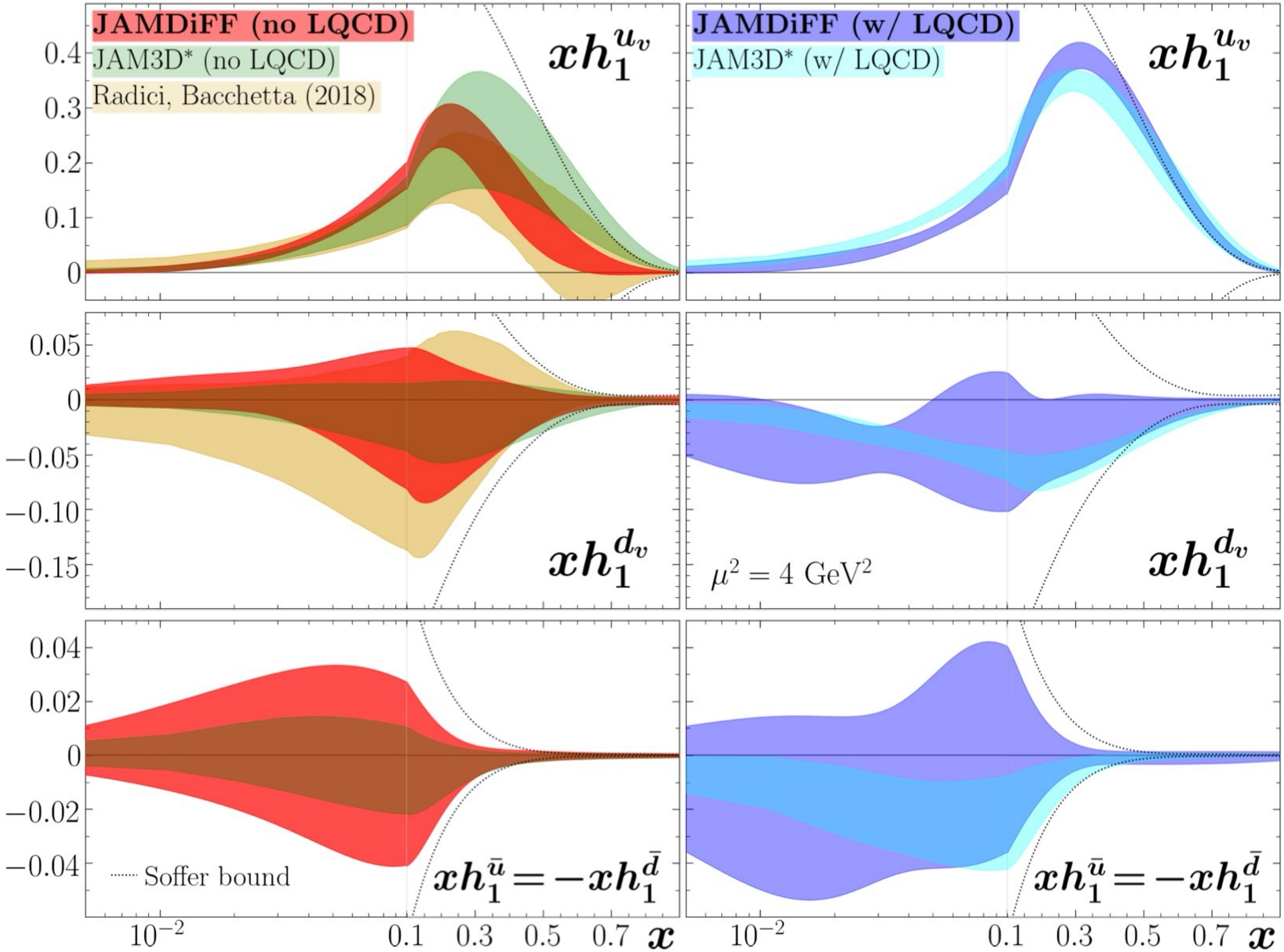

<u>Note</u>: JAM3D* is slightly modified from the published JAM3D-22 version: antiquarks are now included (with $\bar{u} = -\bar{d}$) and $\boldsymbol{\delta}u, \boldsymbol{\delta}d$ from ETMC and PNDME are both included in the fit (rather than just g_T from ETMC)

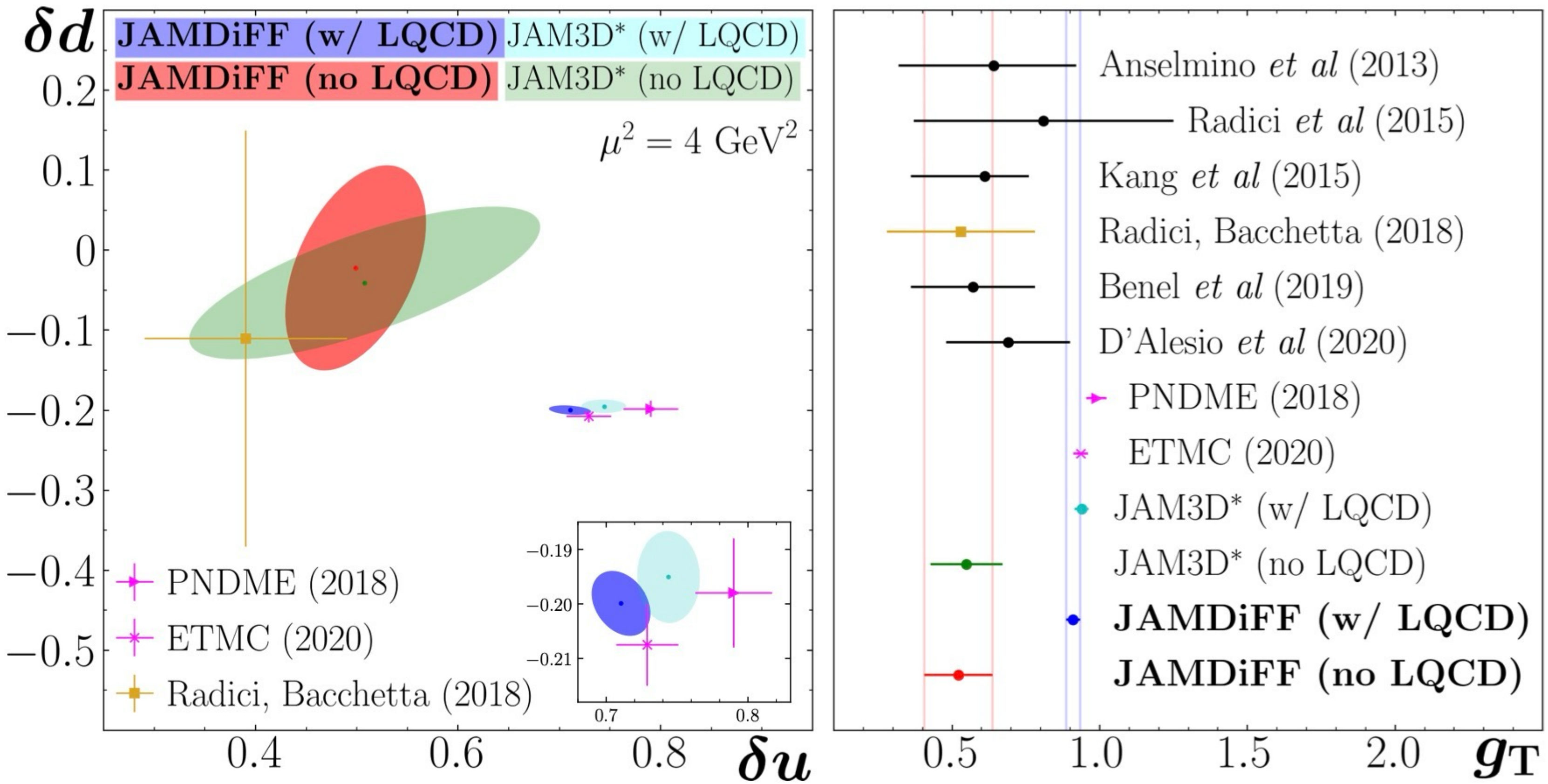

- JAMDiFF (no LQCD) agrees within errors with JAM3D* (no LQCD) and Radici, Bacchetta (2018) for the tensor charges
- Similar to the JAM3D analysis, **JAMDiFF also finds compatibility with lattice once that data is included in the fit (as a Bayesian prior), *and can still describe the experimental data well***

- Possible explanation for the shift (~3-4σ difference with lattice to a ~0.3-2σ difference) in the phenomenological values of the tensor charges once LQCD data is used as a prior:
  - In the no LQCD fit, h_1^{uv} has a maximum and then begins to decrease around where the x coverage of the experimental data ends ($x \approx 0.3$)
  - Within our parameterization, the PDFs fall off smoothly and monotonically as $x \to 1$, and this drives the behavior (and uncertainty) of h_1^{uv} in the unmeasured ($x > 0.3$) region
  - The fit with LQCD included has additional constraints at larger x due to the fact that one integrates from $x \in [0, 1]$ to calculate the tensor charges. This causes h_1^{uv} to now peak at slightly higher $x \approx 0.35$ in order to accommodate both LQCD and experimental data. The Soffer bound forces the with LQCD h_1^{uv} to then decrease shortly after $x = 0.35$ and the PDF again falls off smoothly and monotonically as $x \to 1$
  - **In order to further test the compatibility between LQCD and experimental data, it is of vital importance to have more measurements at larger *x* (for SIDIS) and more forward rapidity (for pp)**
  - The LQCD data and STAR $\sqrt{s}$=200 GeV data have a preference for a larger h_1^{uv} at large x, while the COMPASS proton data and STAR $\sqrt{s}$ = 500 GeV data prefer a smaller h_1^{uv}. In such a situation where there are competing preferences, and we compare analyses containing different subsets of the data, the choice of likelihood function and priors do not guarantee that the fits overlap within statistical uncertainties

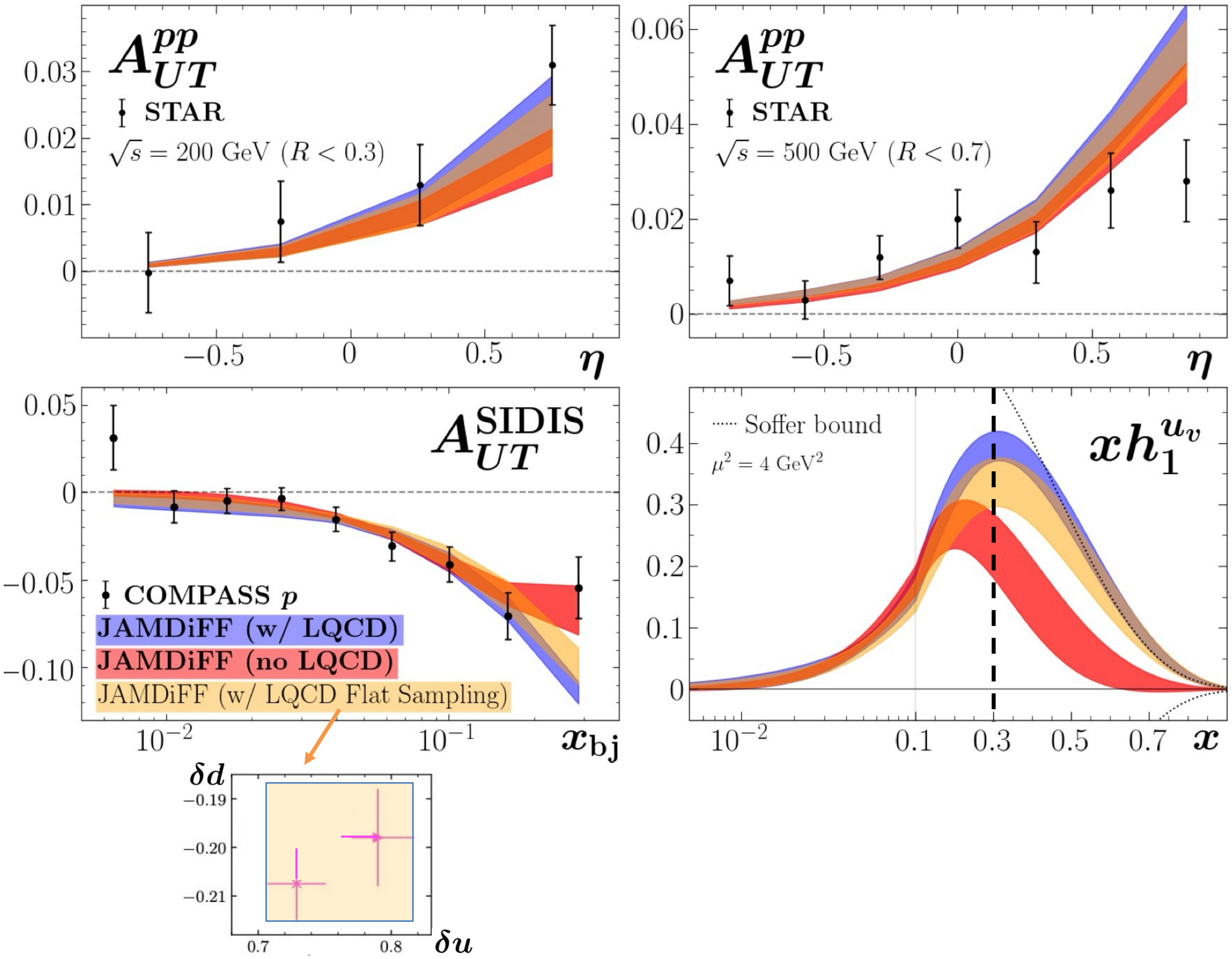
A_{UT}^{pp}
STAR
$\sqrt{s} = 200$ GeV $(R < 0.3)$
0.03
0.02
0.01
0
−0.5
0
0.5
η
0.06
A_{UT}^{pp}
STAR
$\sqrt{s} = 500$ GeV $(R < 0.7)$
0.04
0.02
0
−0.5
0
0.5
η
0.05
A_{UT}^{SIDIS}
0
−0.05
COMPASS p
JAMDiFF (w/ LQCD)
−0.10
JAMDiFF (no LQCD)
JAMDiFF (w/ LQCD Flat Sampling)
10^{-2}
10^{-1}
x_{bj}
Soffer bound
$\mu^2 = 4$ GeV^2
$xh_1^{u_v}$
0.4
0.3
0.2
0.1
0
10^{-2}
0.1
0.3
0.5
0.7
x
δd
−0.19
−0.20
−0.21
0.7
0.8
δu

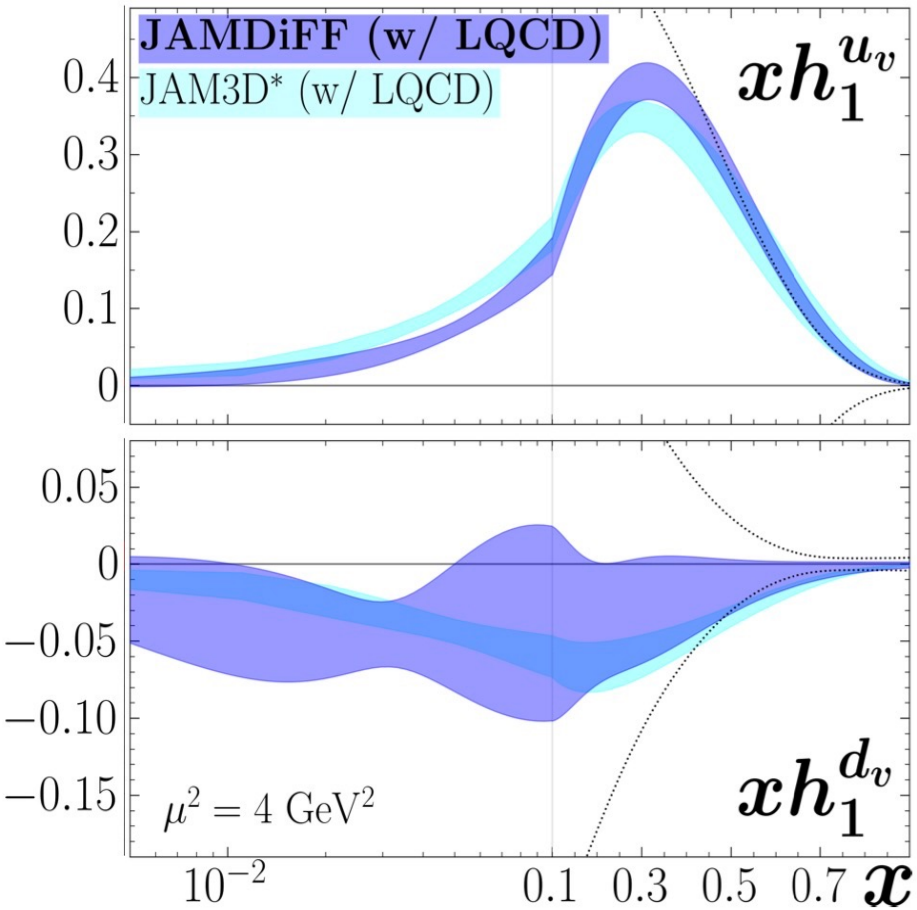

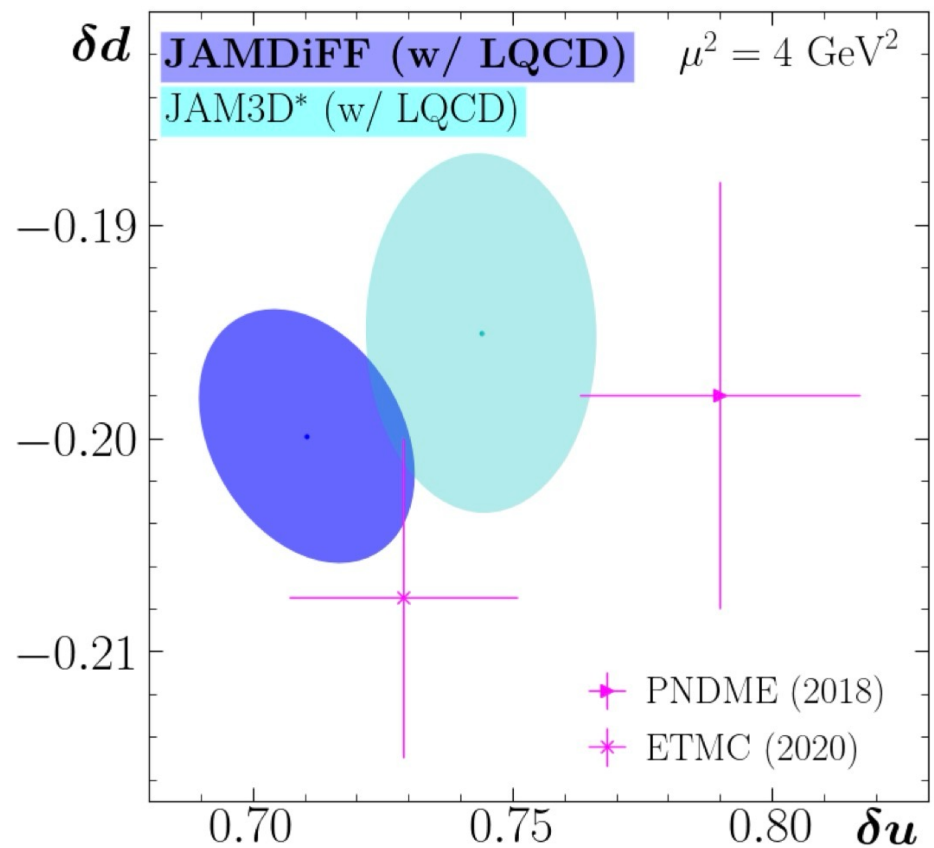

Recent analyses by the JAM Collaboration show agreement between single-hadron and dihadron approaches for extracting transversity as well as compatibility with lattice QCD tensor charges, thus demonstrating the universal nature of all this information

$$D_1^{h_1 h_2/q}(z,\zeta,\vec{k}_T^2,\vec{R}_T^2,\vec{k}_T\cdot\vec{R}_T) = \frac{\boldsymbol{z}}{\boldsymbol{32\pi^3(1-\zeta^2)}}\,\mathrm{Tr}\Big[\Delta^{h_1 h_2/q}(z,\vec{k}_T;P_1,P_2)\gamma^-\Big]$$

NEW definition of dihadron FFs

$$D_1^{h_1 h_2/q}(z,\zeta,\vec{k}_T^2,\vec{R}_T^2,\vec{k}_T\cdot\vec{R}_T) = \frac{\boldsymbol{z}}{\boldsymbol{32\pi^3(1-\zeta^2)}}\mathrm{Tr}\left[\Delta^{h_1 h_2/q}(z,\vec{k}_T;P_1,P_2)\gamma^-\right]$$

$$\sum_{h_1}\sum_{h_2}\int dz\,d\zeta\,d^2\vec{k}_T\,d^2\vec{R}_T\,D_1^{h_1 h_2/q}(z,\zeta,\vec{k}_T^2,\vec{R}_T^2,\vec{k}_T\cdot\vec{R}_T) = \underbrace{\langle\mathcal{N}(\mathcal{N}-1)\rangle}$$

Expectation value for the total number of *hadron pairs* produced when the parton fragments

Note: Recent papers by Collins, Rogers (2024) and Rogers, Courtoy (2024) do *not* actually put into question our results regarding our DiFF definition being a number density.

$$D_1^{h_1 h_2/q}(z,\zeta,\vec{k}_T^2,\vec{R}_T^2,\vec{k}_T\cdot\vec{R}_T) = \frac{z}{32\pi^3(1-\zeta^2)}\mathrm{Tr}\left[\Delta^{h_1h_2/q}(z,\vec{k}_T;P_1,P_2)\gamma^-\right]$$

$$\sum_{h_1}\sum_{h_2}\int dz\, d\zeta\, d^2\vec{k}_T\, d^2\vec{R}_T\, D_1^{h_1 h_2/q}(z,\zeta,\vec{k}_T^2,\vec{R}_T^2,\vec{k}_T\cdot\vec{R}_T) = \underbrace{\langle \mathcal{N}(\mathcal{N}-1)\rangle}$$

Expectation value for the total number of *hadron pairs* produced when the parton fragments

Note: Recent papers by Collins, Rogers (2024) and Rogers, Courtoy (2024) do *not* actually put into question our results regarding our DiFF definition being a number density.

$$e^+e^- \to (h_1 h_2)\,X$$

$$\frac{d\sigma}{dz\,d\zeta\,d^2\vec{R}_T} = \sum_q \boxed{\frac{4\pi N_c \alpha_{\rm em}^2}{3Q^2}\, e_q^2}\, D_1^{h_1h_2/q}(z,\zeta,\vec{R}_T^2)$$

total partonic cross section for $e^+e^- \to \gamma \to q\bar{q} \equiv \hat{\sigma}_0^q$

$$D_1^{h_1 h_2/q}(z,\zeta,\vec{k}_T^2,\vec{R}_T^2,\vec{k}_T\cdot\vec{R}_T) = \frac{z}{32\pi^3(1-\zeta^2)}\mathrm{Tr}\left[\Delta^{h_1 h_2/q}(z,\vec{k}_T;P_1,P_2)\gamma^-\right]$$

$$\sum_{h_1}\sum_{h_2}\int dz\,d\zeta\,d^2\vec{k}_T\,d^2\vec{R}_T\,D_1^{h_1 h_2/q}(z,\zeta,\vec{k}_T^2,\vec{R}_T^2,\vec{k}_T\cdot\vec{R}_T) = \underbrace{\langle\mathcal{N}(\mathcal{N}-1)\rangle}$$

Expectation value for the total number of *hadron pairs* produced when the parton fragments

Note: Recent papers by Collins, Rogers (2024) and Rogers, Courtoy (2024) do *not* actually put into question our results regarding our DiFF definition being a number density.

$e^+e^-\to(h_1h_2)\,X$

$$\frac{d\sigma}{dz\,d\zeta\,d^2\vec{R}_T} = \sum_q \frac{4\pi N_c\alpha_{\rm em}^2}{3Q^2}\,e_q^2\,D_1^{h_1h_2/q}(z,\zeta,\vec{R}_T^2)$$

total partonic cross section for $e^+e^-\to\gamma\to q\bar{q}\equiv\hat{\sigma}_0^q$

$e^+e^-\to h\,X$

$$\frac{d\sigma}{dz} = \sum_q \hat{\sigma}_0^q\,D_1^{h/q}(z)$$

This is exactly the structure *dσ* should have if D_1 has a number density interpretation (alternative definitions would introduce additional factors that don't give the expected parton model result)

$$D_1^{h_1 h_2/q}(z,\zeta,\vec{k}_T^2,\vec{R}_T^2,\vec{k}_T\cdot\vec{R}_T) = \frac{z}{32\pi^3(1-\zeta^2)}\mathrm{Tr}\left[\Delta^{h_1 h_2/q}(z,\vec{k}_T;P_1,P_2)\gamma^-\right]$$

$$\sum_{h_1}\sum_{h_2}\int dz\, d\zeta\, d^2\vec{k}_T\, d^2\vec{R}_T\, D_1^{h_1 h_2/q}(z,\zeta,\vec{k}_T^2,\vec{R}_T^2,\vec{k}_T\cdot\vec{R}_T) = \underbrace{\langle \mathcal{N}(\mathcal{N}-1)\rangle}$$

Expectation value for the total number of *hadron pairs* produced when the parton fragments

Note: Recent papers by Collins, Rogers (2024) and Rogers, Courtoy (2024) do *not* actually put into question our results regarding our DiFF definition being a number density.

$e^+e^- \to (h_1 h_2)\, X$

$$\frac{d\sigma}{dz\, d\zeta\, d^2\vec{R}_T} = \sum_q \frac{4\pi N_c \alpha_{\rm em}^2}{3Q^2}\, e_q^2\, D_1^{h_1 h_2/q}(z,\zeta,\vec{R}_T^2)$$

total partonic cross section for $e^+e^- \to \gamma \to q\bar{q} \equiv \hat{\sigma}_0^q$

$e^+e^- \to h\, X$

$$\frac{d\sigma}{dz} = \sum_q \hat{\sigma}_0^q\, D_1^{h/q}(z)$$

$$\boldsymbol{D_1^{h_1 h_2/i}(w,x,\vec{Y}^2,\vec{Z}^2,\vec{Y}\cdot\vec{Z})} \equiv \mathcal{J}\cdot D_1^{h_1 h_2/i}(z,\zeta,\vec{k}_T^2,\vec{R}_T^2,\vec{k}_T\cdot\vec{R}_T)$$

is a number density

Jacobian for the variable transformation

DiFFs extracted from experiment now have a clear physical meaning: they are densities in the momentum variables for the number of hadron pairs ($h_1 h_2$) fragmenting from the parton

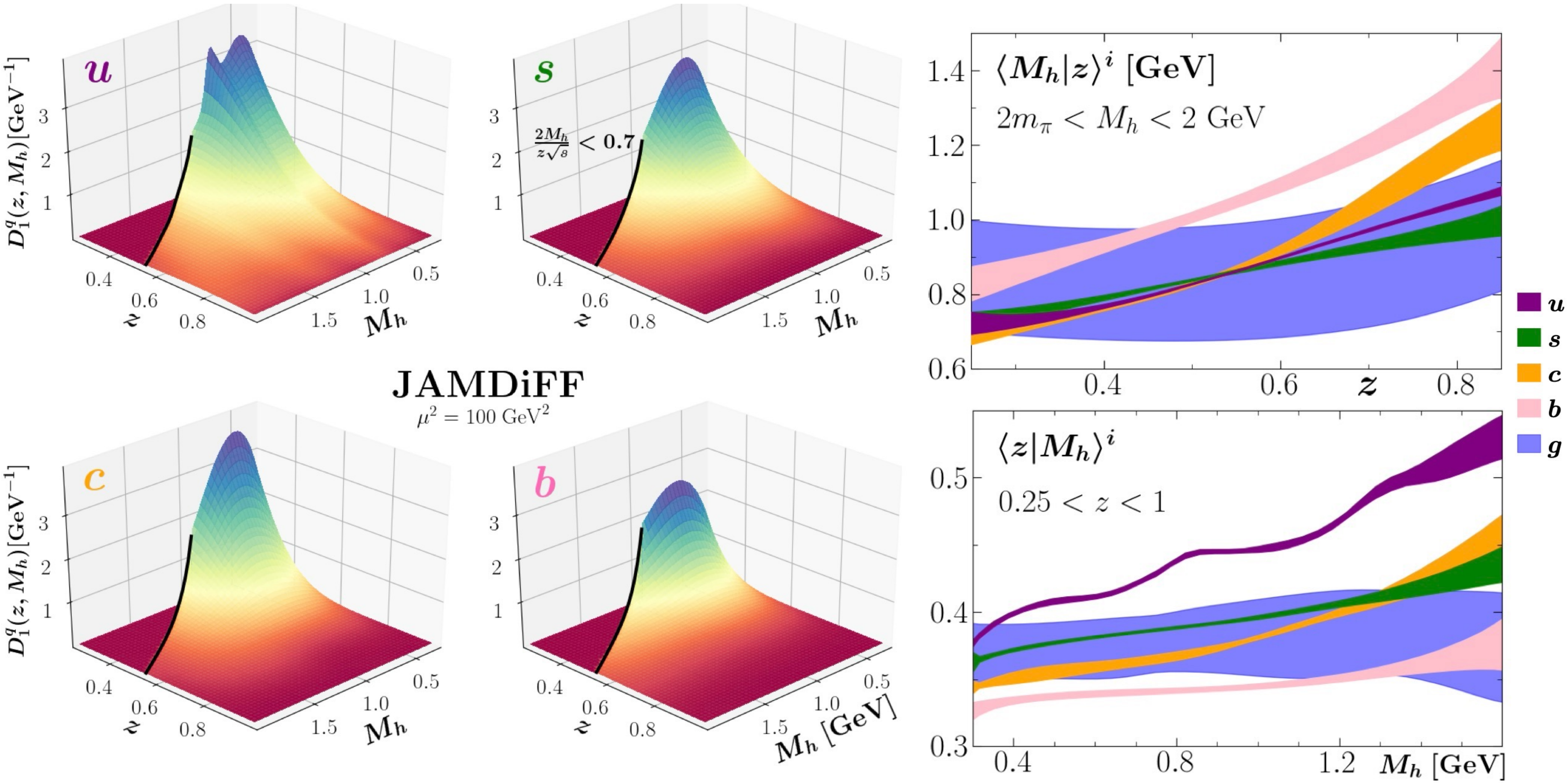

Summary

- We have performed separate QCD global analyses of TSSAs in TMD/collinear twist-3 single-hadron observables and in dihadron fragmentation measurements, also studying the role of lattice QCD in our fits. Work is in progress combining JAM3D and JAMDiFF that will also incorporate Collins hadron-in-jet data and new COMPASS SIDIS (Sivers, Collins) and DY (Sivers) measurements.

- We have introduced a new definition of dihadron fragmentation functions that is consistent with a number density interpretation, allowing for a clear physical interpretation of our extracted DiFFs

- Quantities of particular interest are the tensor charges of the nucleon - they are fundamental properties of the nucleon that have connections to QCD phenomenology, lattice QCD computations, model calculations, and low-energy beyond the Standard Model studies (e.g., beta decay, EDM)

Recent analyses by the JAM Collaboration show agreement between single-hadron and dihadron approaches for extracting transversity as well as compatibility with lattice QCD tensor charges, thus demonstrating the universal nature of all this information

Backup Slides

- Parameterization of the $\pi^+\pi^-$ DiFFs $\boldsymbol{D_1(z, M_h)}$, $\boldsymbol{H_1^{\sphericalangle}(z, M_h)}$

  - Symmetry relations (Courtoy, et al. (2012))

$$D_1^u = D_1^d = D_1^{\bar{u}} = D_1^{\bar{d}}, \qquad H_1^{\sphericalangle,u} = -H_1^{\sphericalangle,d} = -H_1^{\sphericalangle,\bar{u}} = H_1^{\sphericalangle,\bar{d}},$$

$$D_1^s = D_1^{\bar{s}}, \quad D_1^c = D_1^{\bar{c}}, \quad D_1^b = D_1^{\bar{b}} \qquad H_1^{\sphericalangle,s} = -H_1^{\sphericalangle,\bar{s}} = H_1^{\sphericalangle,c} = -H_1^{\sphericalangle,\bar{c}} = 0$$

also have D_1^g

  - Positivity bounds (Bacchetta, Radici (2003))

$$D_1(z, M_h) > 0 \qquad |H_1^{\sphericalangle}(z, M_h)| < D_1(z, M_h)$$

- Parameterization of the $\pi^+\pi^-$ DiFFs $\boldsymbol{D_1(z, M_h)}$, $\boldsymbol{H_1^{\sphericalangle}(z, M_h)}$
  - Because of the resonance structure of the e^+e^- cross section, we use a grid in M_h whose density depends on the flavor and DiFF and then at each grid point we have the functional form $\sim N z^a (1-z)^b$. The grid is then interpolated to give a general M_h dependence. E.g., for the up quark for D_1,

$$\mathbf{M}_h^u = [2m_\pi, 0.40, 0.50, 0.70, 0.75, 0.80, 0.90, 1.00, 1.20, 1.30, 1.40, 1.60, 1.80, 2.00]\ \text{GeV}$$

$$D_1^u(z, \mathbf{M}_h^{u,i}) = \sum_{j=1,2,3} \frac{N_{ij}^u z^{\alpha_{ij}^u} (1-z)^{\beta_{ij}^u}}{\mathrm{B}[\alpha_{ij}^u + 1, \beta_{ij}^u + 1]}$$

$\rightarrow$ 204 parameters for D_1 and 48 parameters for $H_1^{\sphericalangle}$

- Parameterization of the $\pi^+\pi^-$ DiFFs $D_1(z, M_h)$, $H_1^{\sphericalangle}(z, M_h)$

  - Because of the resonance structure of the e^+e^- cross section, we use a grid in M_h whose density depends on the flavor and DiFF and then at each grid point we have the functional form $\sim N z^a (1-z)^b$. The grid is then interpolated to give a general M_h dependence. E.g., for the up quark for D_1,

$$\mathbf{M}_h^u = [2m_\pi, 0.40, 0.50, 0.70, 0.75, 0.80, 0.90, 1.00, 1.20, 1.30, 1.40, 1.60, 1.80, 2.00] \text{ GeV}$$

$$D_1^u(z, \mathbf{M}_h^{u,i}) = \sum_{j=1,2,3} \frac{N_{ij}^u z^{\alpha_{ij}^u} (1-z)^{\beta_{ij}^u}}{\mathrm{B}[\alpha_{ij}^u + 1, \beta_{ij}^u + 1]}$$

$\rightarrow$ 204 parameters for D_1 and 48 parameters for $H_1^{\sphericalangle}$

  - The Belle data is not sufficient to perform a flavor separation for D_1, so we supplement with data from Pythia for σ^q/σ^{tot} for $q = s, c, b$ at

$$\sqrt{s} = [10.58, 30.73, 50.88, 71.04, 91.19] \text{ GeV}$$

using different tunes to quantify systematic uncertainties

$\rightarrow$ constrain D_1 for s, c, b as well as the gluon through scaling violations

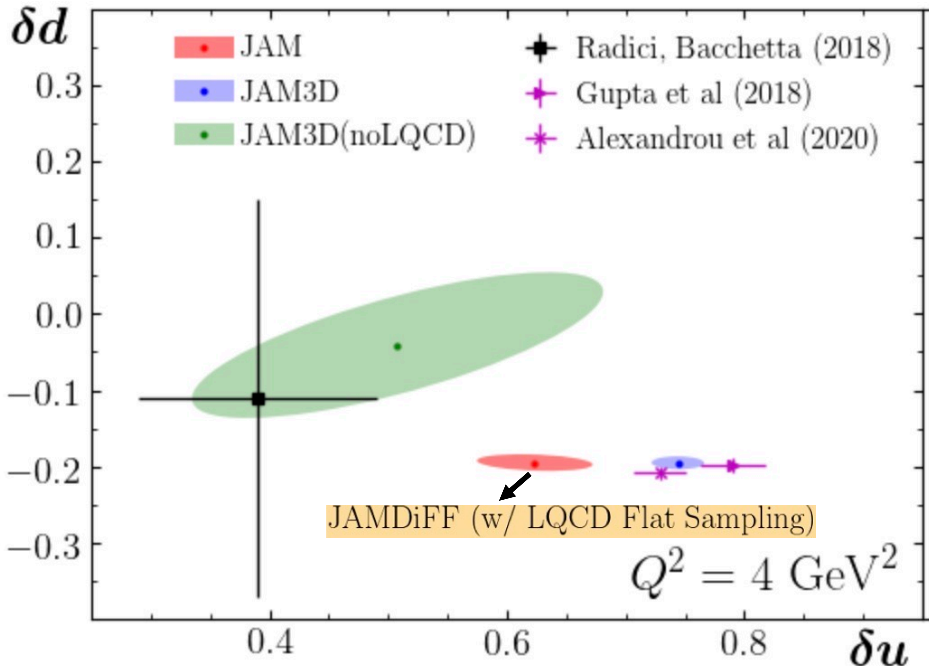
δd
0.3
0.2
0.1
0.0
−0.1
−0.2
−0.3
0.4
0.6
0.8
δu
JAM
JAM3D
JAM3D(noLQCD)
Radici, Bacchetta (2018)
Gupta et al (2018)
Alexandrou et al (2020)
JAMDiFF (w/ LQCD Flat Sampling)
Q² = 4 GeV²

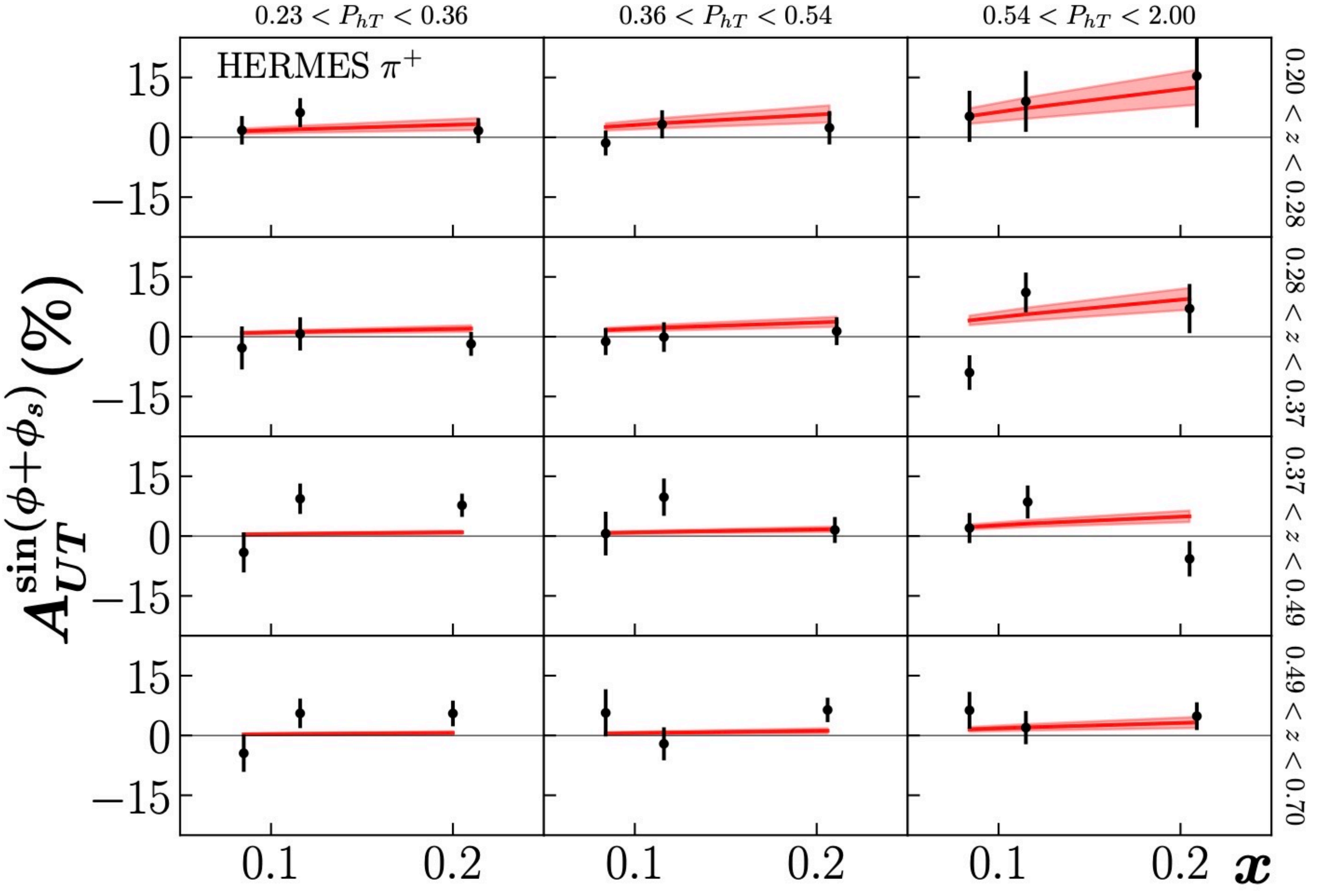
$0.23 < P_{hT} < 0.36$
$0.36 < P_{hT} < 0.54$
$0.54 < P_{hT} < 2.00$
HERMES π^+
$A_{UT}^{\sin(\phi+\phi_s)}$ (%)
15
0
−15
0.1
0.2
x
$0.20 < z < 0.28$
$0.28 < z < 0.37$
$0.37 < z < 0.49$
$0.49 < z < 0.70$

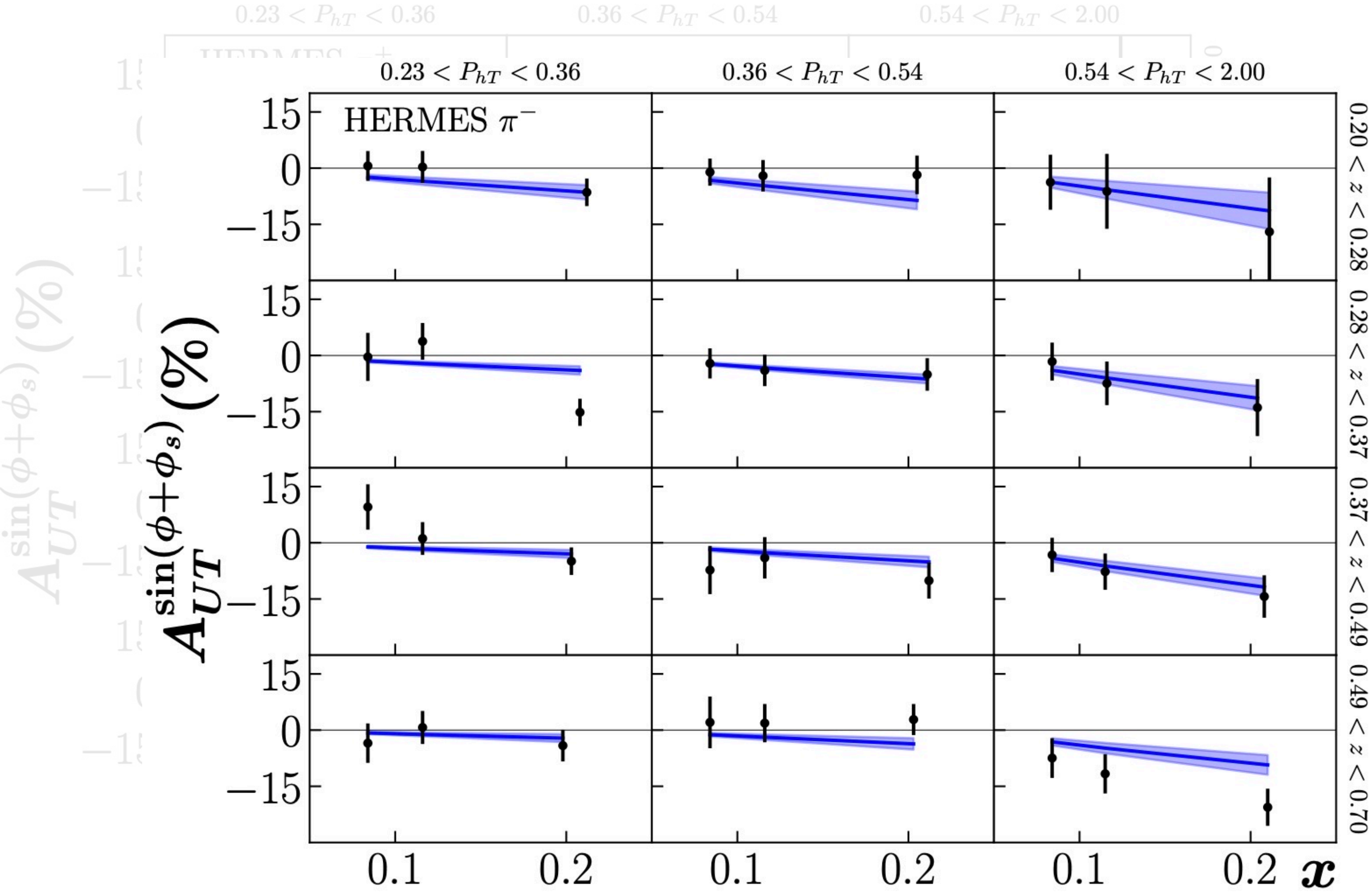
0.23 < P_{hT} < 0.36
0.36 < P_{hT} < 0.54
0.54 < P_{hT} < 2.00
HERMES π^-
$A_{UT}^{\sin(\phi+\phi_s)}$ (%)
15
0
−15
0.1
0.2
x
0.20 < z < 0.28
0.28 < z < 0.37
0.37 < z < 0.49
0.49 < z < 0.70

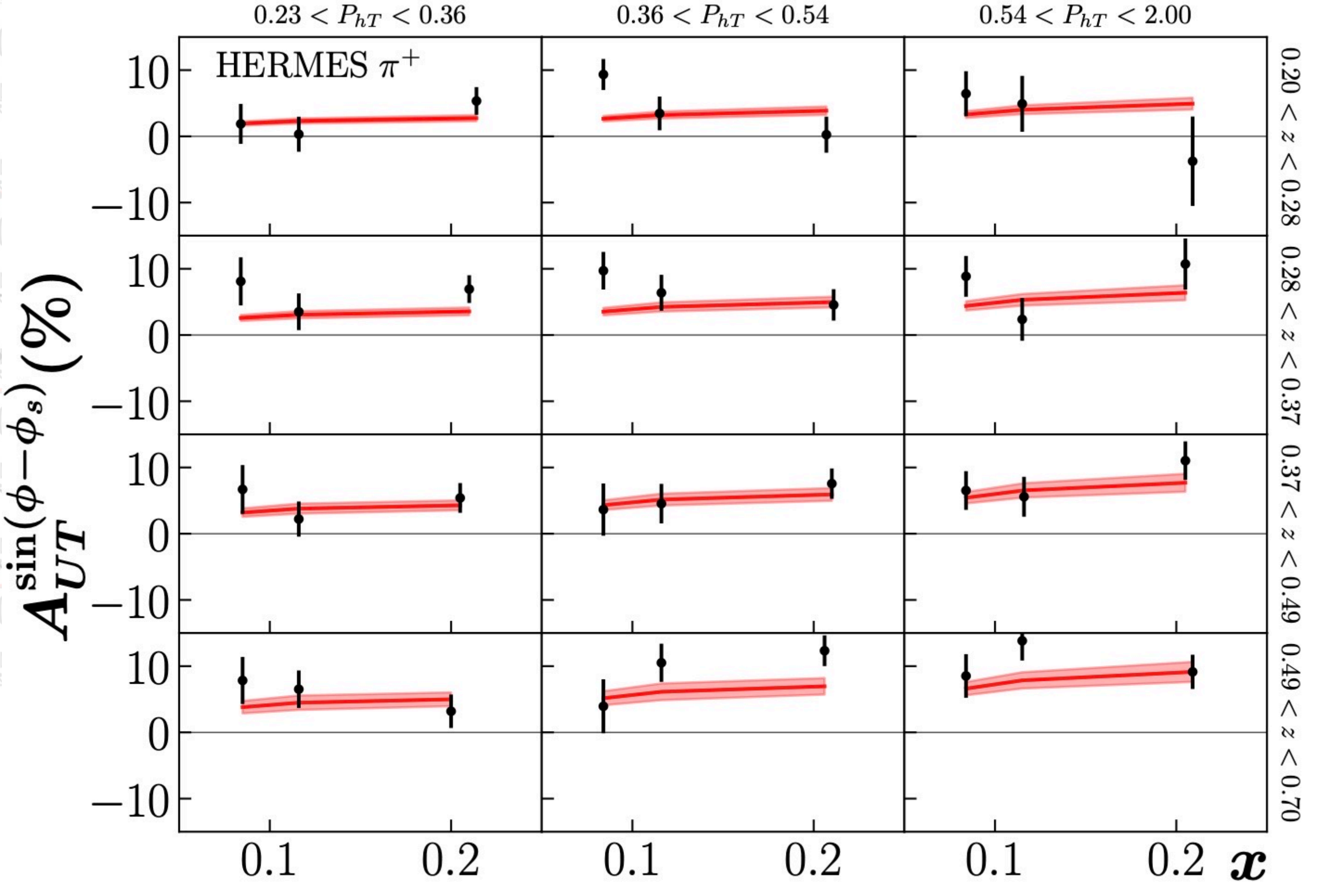
$0.23 < P_{hT} < 0.36$
$0.36 < P_{hT} < 0.54$
$0.54 < P_{hT} < 2.00$
HERMES π^+
$A_{UT}^{\sin(\phi-\phi_s)}$ (%)
$0.20 < z < 0.28$
$0.28 < z < 0.37$
$0.37 < z < 0.49$
$0.49 < z < 0.70$
10
0
−10
0.1
0.2
x

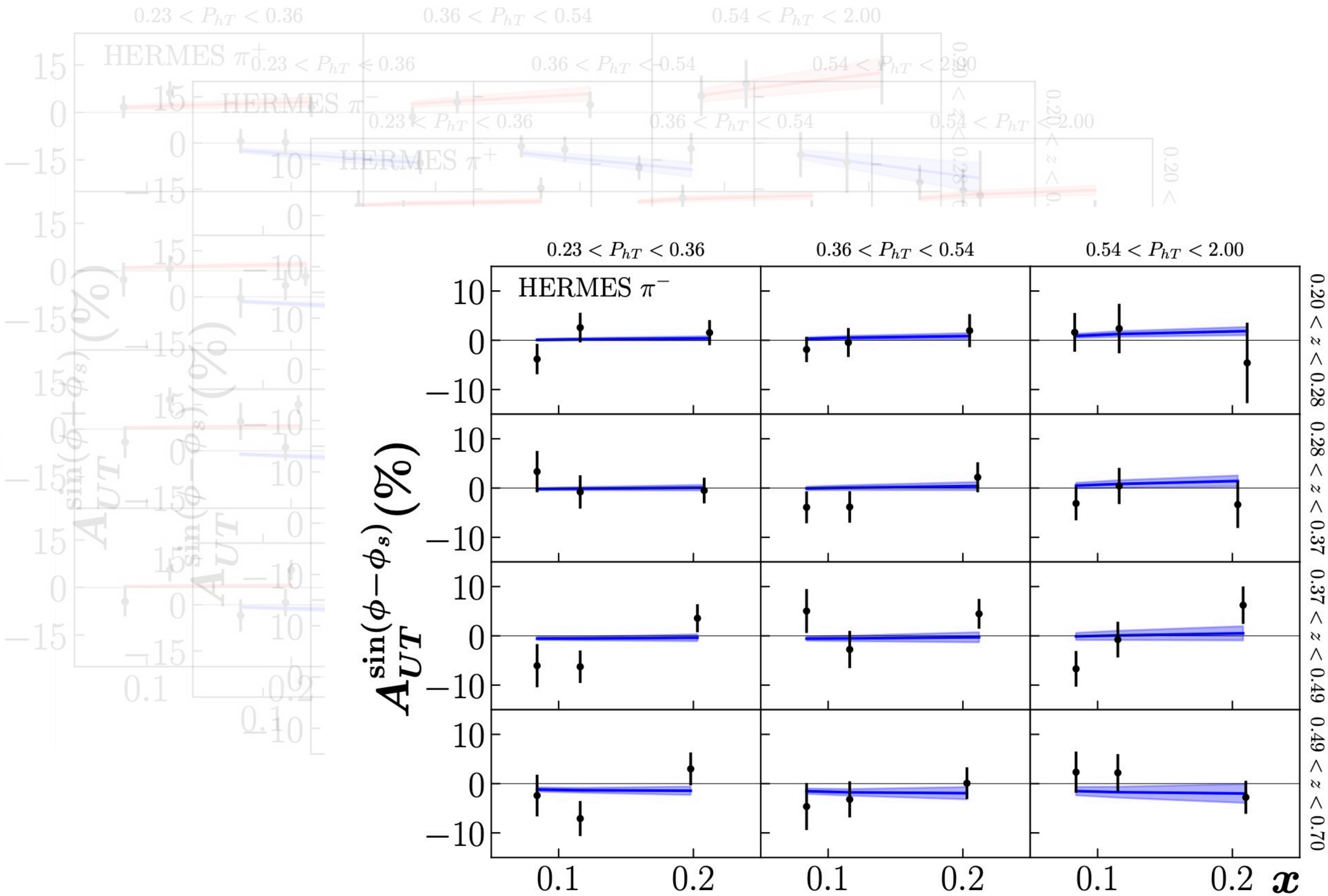
0.23 < P_{hT} < 0.36
0.36 < P_{hT} < 0.54
0.54 < P_{hT} < 2.00
HERMES π^-
$A_{UT}^{\sin(\phi-\phi_s)}$ (%)
0.20 < z < 0.28
0.28 < z < 0.37
0.37 < z < 0.49
0.49 < z < 0.70
10
0
−10
0.1
0.2
x

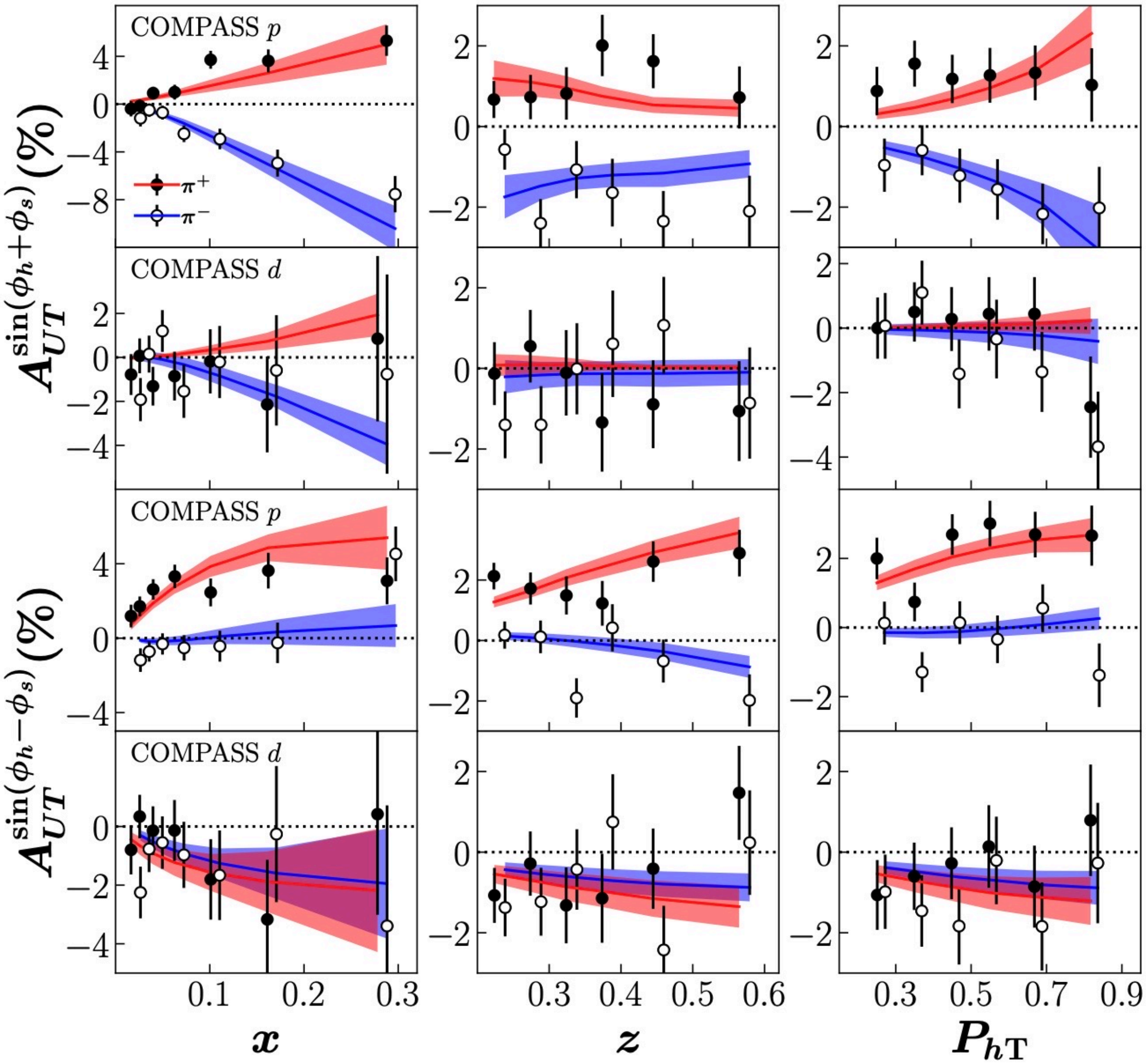
COMPASS p
COMPASS d
COMPASS p
COMPASS d
π^+
π^-
$A_{UT}^{\sin(\phi_h+\phi_s)}$ (%)
$A_{UT}^{\sin(\phi_h-\phi_s)}$ (%)
x
z
P_{hT}

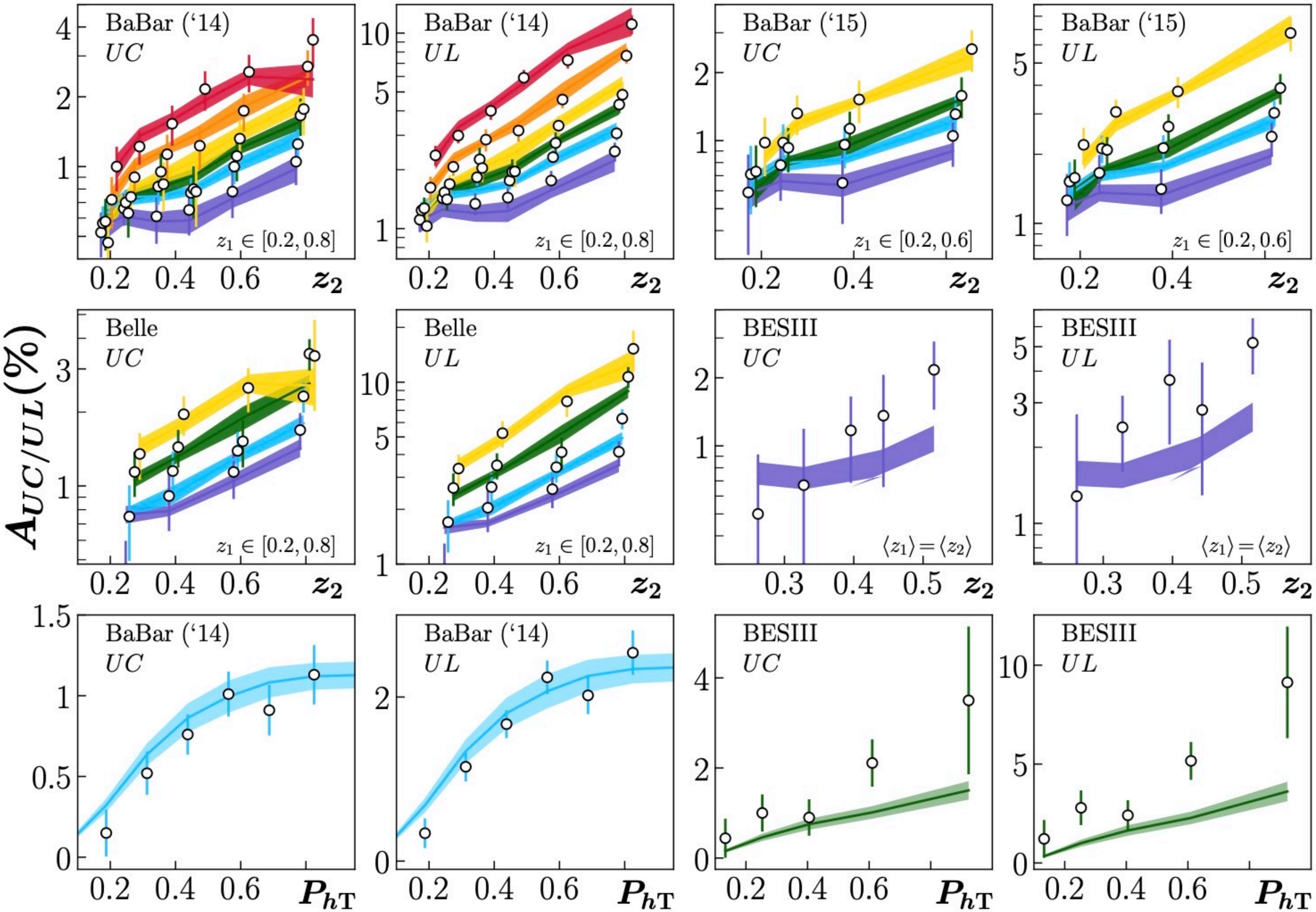
BaBar ('14)
UC
BaBar ('14)
UL
BaBar ('15)
UC
BaBar ('15)
UL
Belle
UC
Belle
UL
BESIII
UC
BESIII
UL
$z_1 \in [0.2, 0.8]$
$z_1 \in [0.2, 0.6]$
$\langle z_1 \rangle = \langle z_2 \rangle$
$A_{UC/UL}(\%)$
z_2
P_{hT}

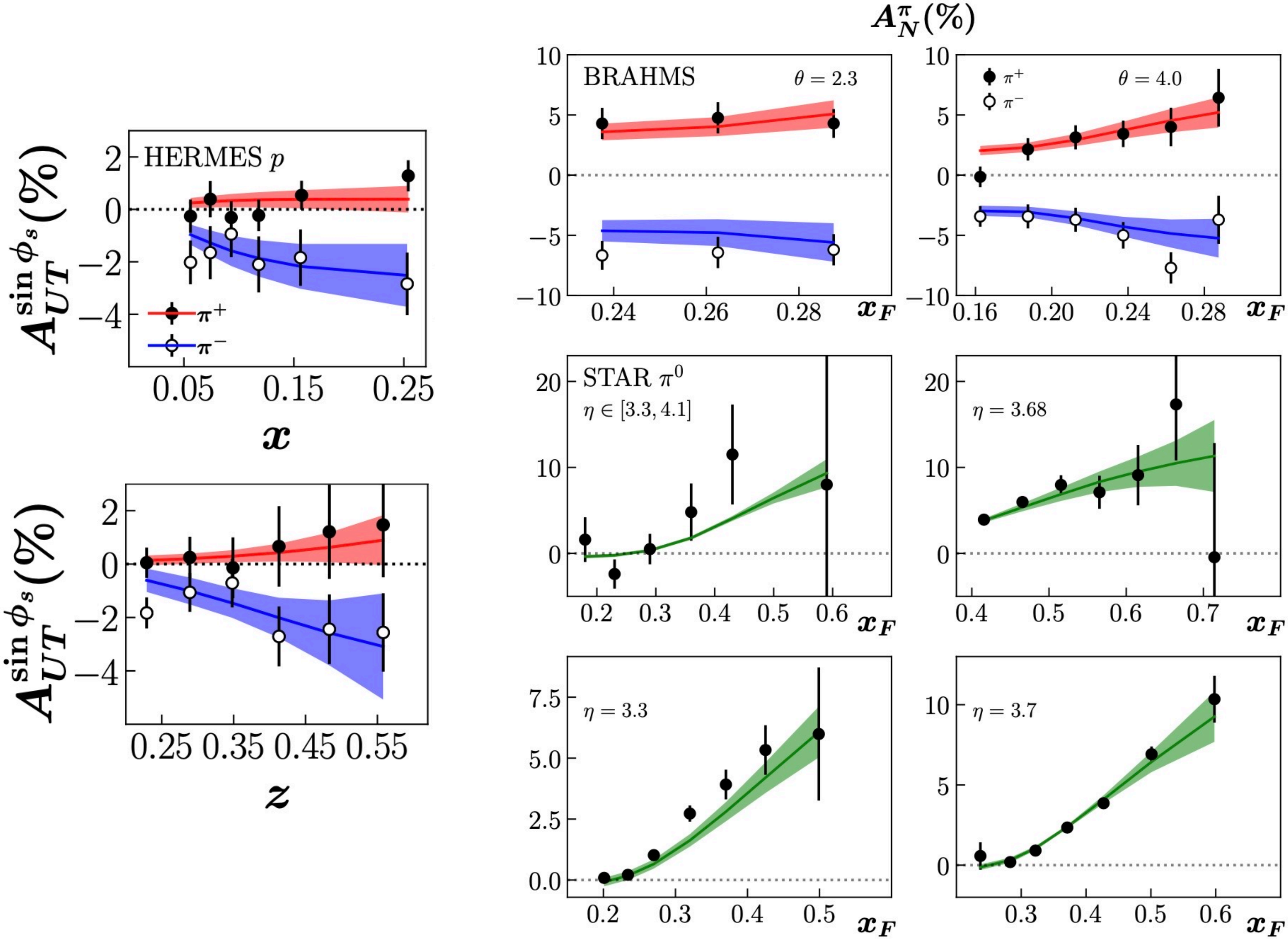
$A_N^{\pi}(\%)$
HERMES p
$A_{UT}^{\sin\phi_s}(\%)$
π^+
π^-
x
z
BRAHMS
$\theta = 2.3$
$\theta = 4.0$
STAR π^0
$\eta \in [3.3, 4.1]$
$\eta = 3.68$
$\eta = 3.3$
$\eta = 3.7$
x_F

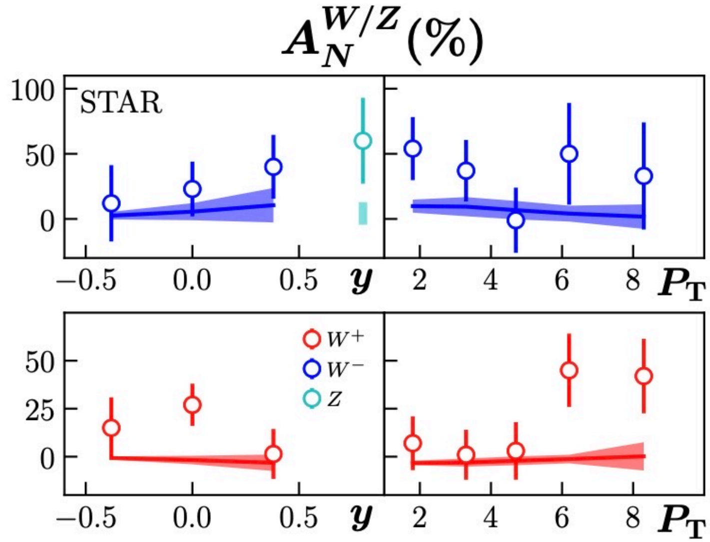
$A_N^{W/Z}$ (%)
STAR
W^+
W^-
Z
y
P_T

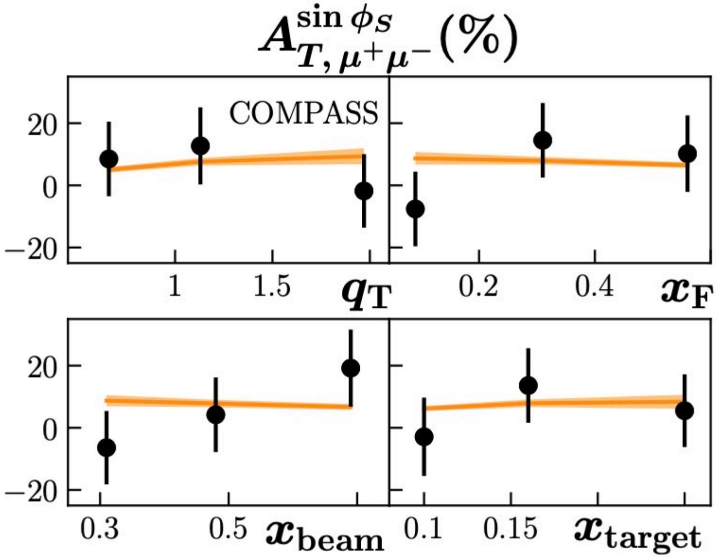
$A_{T,\mu^+\mu^-}^{\sin\phi_S}$ (%)
COMPASS
q_T
x_F
x_{beam}
x_{target}

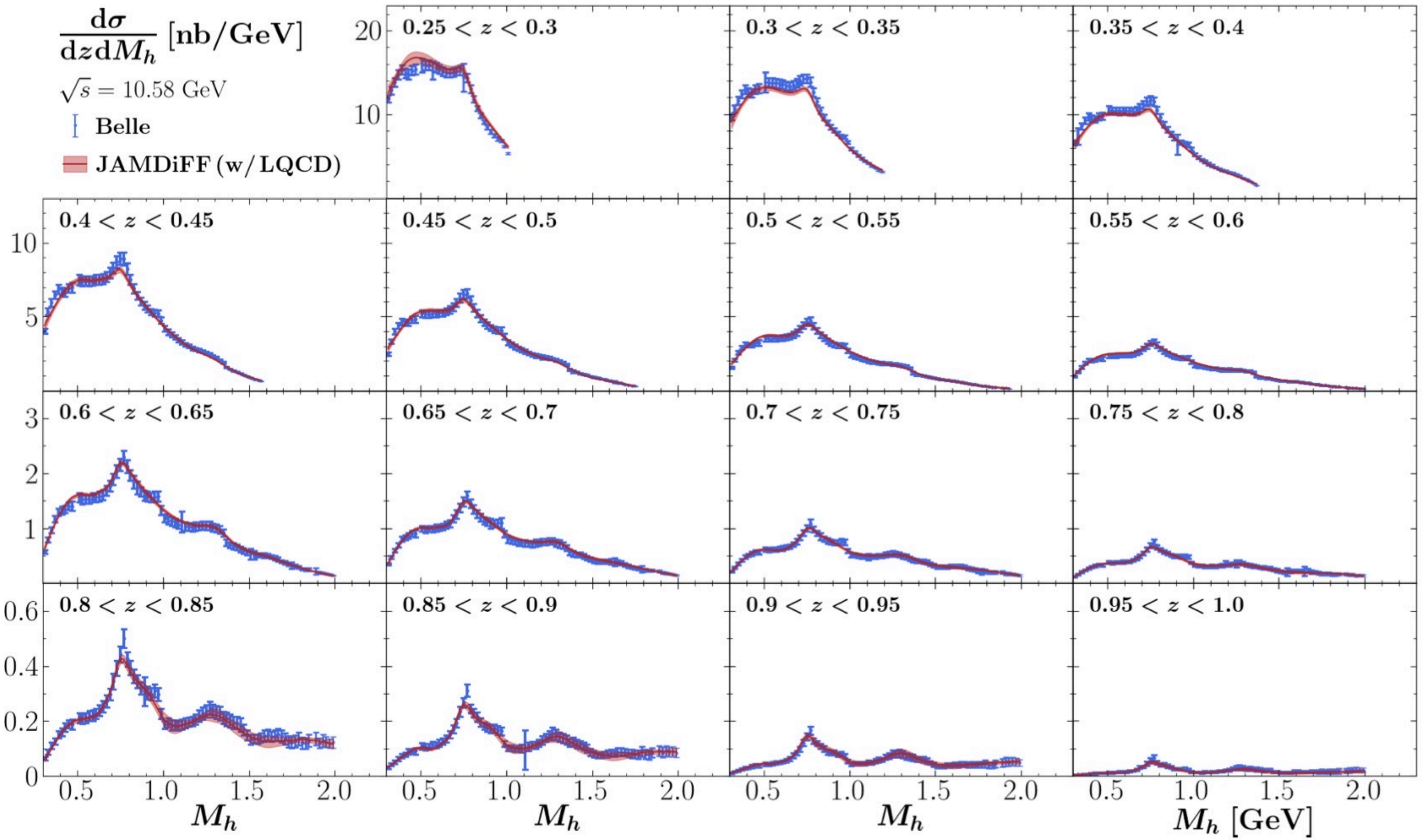
$\frac{d\sigma}{dz dM_h}$ [nb/GeV]
$\sqrt{s} = 10.58$ GeV
Belle
JAMDiFF (w/ LQCD)
$0.25 < z < 0.3$
$0.3 < z < 0.35$
$0.35 < z < 0.4$
$0.4 < z < 0.45$
$0.45 < z < 0.5$
$0.5 < z < 0.55$
$0.55 < z < 0.6$
$0.6 < z < 0.65$
$0.65 < z < 0.7$
$0.7 < z < 0.75$
$0.75 < z < 0.8$
$0.8 < z < 0.85$
$0.85 < z < 0.9$
$0.9 < z < 0.95$
$0.95 < z < 1.0$
M_h
M_h [GeV]

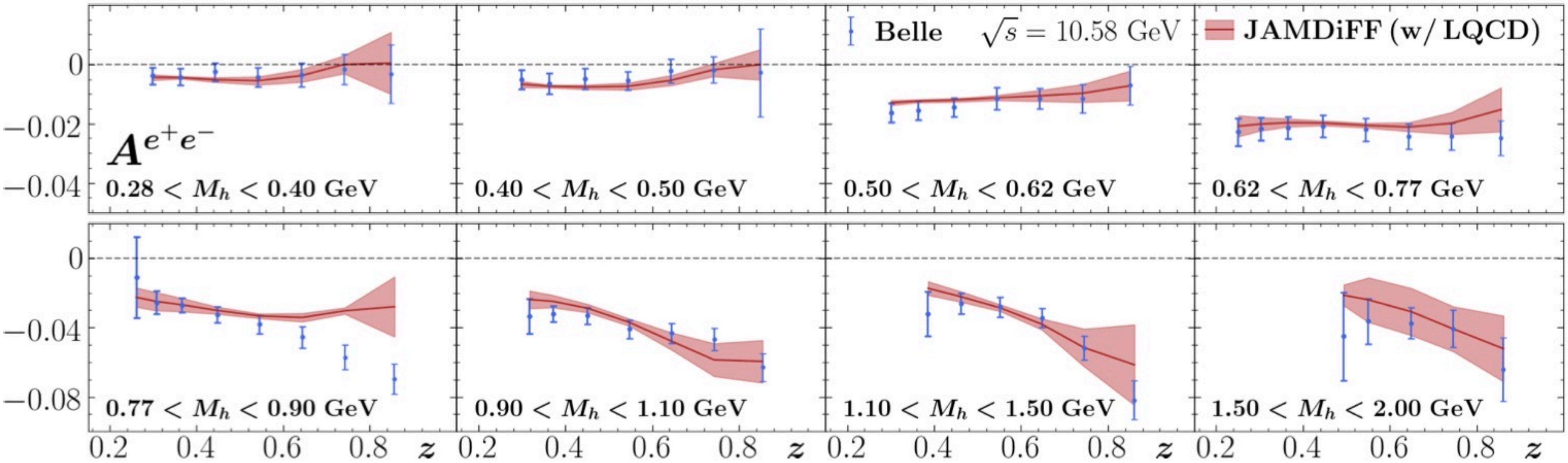
Belle $\sqrt{s} = 10.58$ GeV
JAMDiFF (w/ LQCD)
$A^{e^+e^-}$
$0.28 < M_h < 0.40$ GeV
$0.40 < M_h < 0.50$ GeV
$0.50 < M_h < 0.62$ GeV
$0.62 < M_h < 0.77$ GeV
$0.77 < M_h < 0.90$ GeV
$0.90 < M_h < 1.10$ GeV
$1.10 < M_h < 1.50$ GeV
$1.50 < M_h < 2.00$ GeV
z

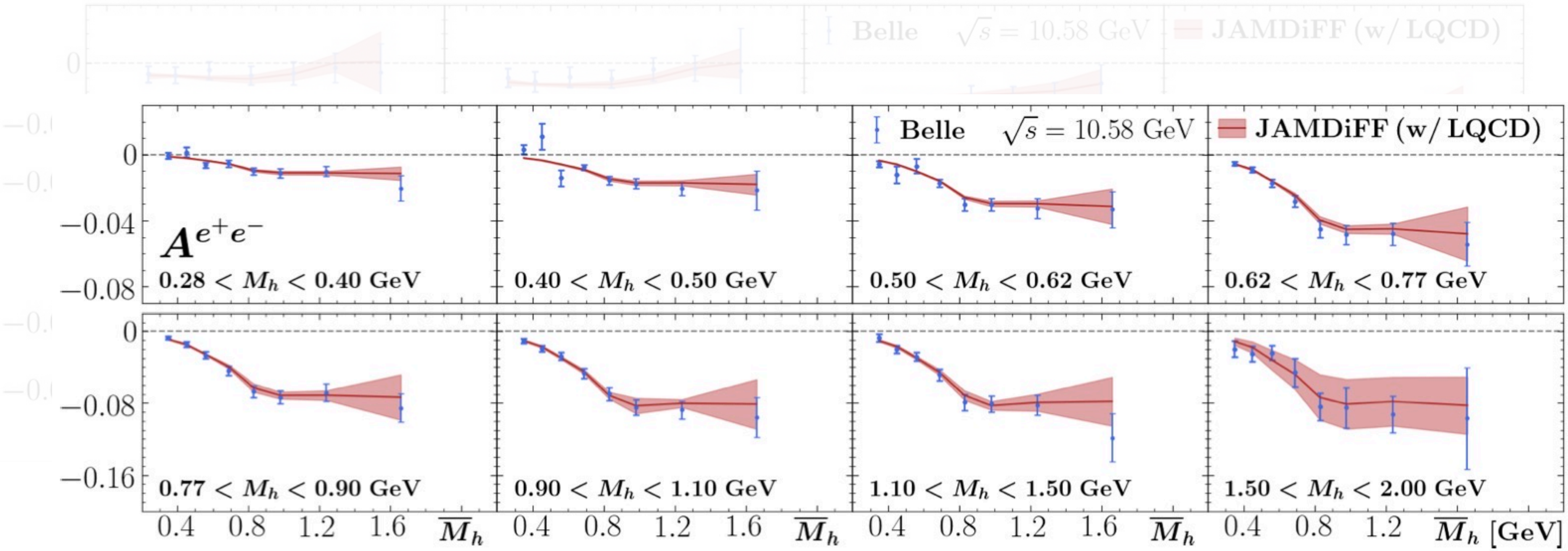
Belle $\sqrt{s} = 10.58$ GeV
JAMDiFF (w/ LQCD)
$A^{e^+e^-}$
0
−0.04
−0.08
−0.16
$0.28 < M_h < 0.40$ GeV
$0.40 < M_h < 0.50$ GeV
$0.50 < M_h < 0.62$ GeV
$0.62 < M_h < 0.77$ GeV
$0.77 < M_h < 0.90$ GeV
$0.90 < M_h < 1.10$ GeV
$1.10 < M_h < 1.50$ GeV
$1.50 < M_h < 2.00$ GeV
0.4
0.8
1.2
1.6
$\overline{M}_h$ [GeV]

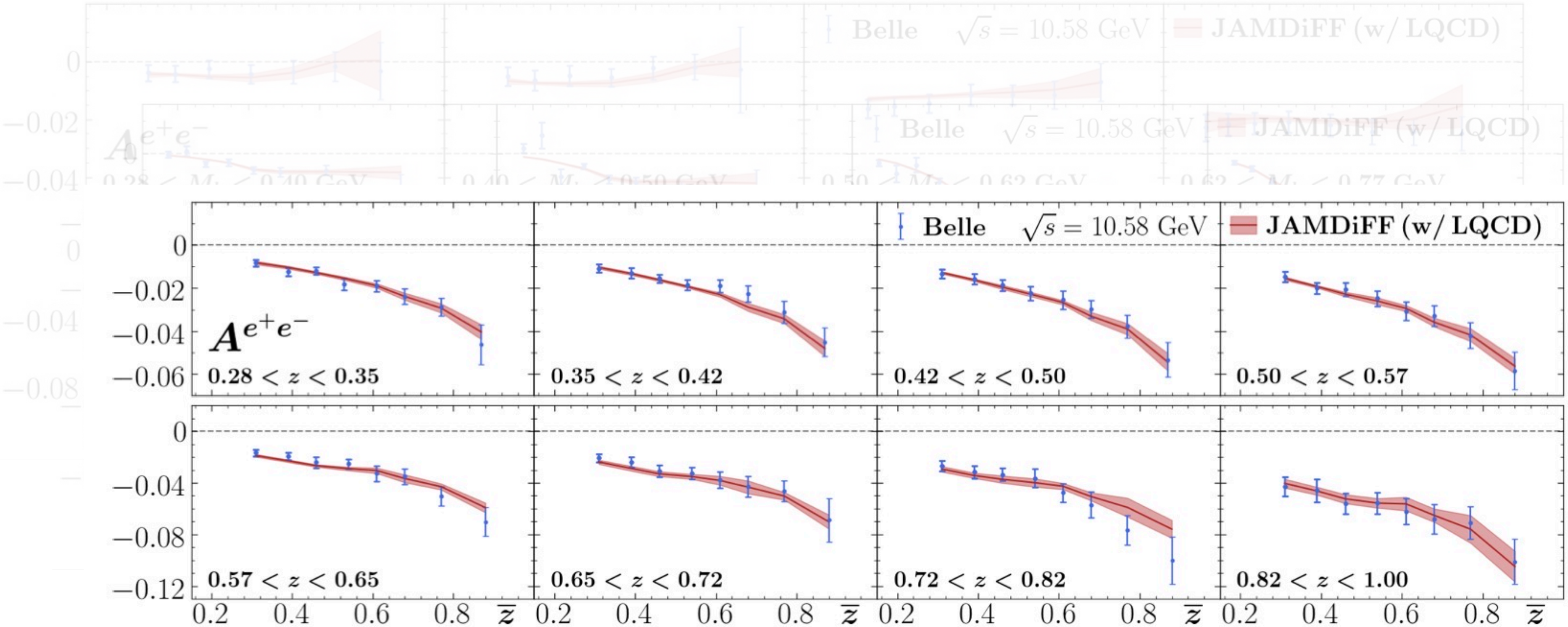
Belle $\sqrt{s} = 10.58$ GeV
JAMDiFF (w/ LQCD)
$A^{e^+e^-}$
$0.28 < z < 0.35$
$0.35 < z < 0.42$
$0.42 < z < 0.50$
$0.50 < z < 0.57$
$0.57 < z < 0.65$
$0.65 < z < 0.72$
$0.72 < z < 0.82$
$0.82 < z < 1.00$
0
−0.02
−0.04
−0.06
−0.08
−0.12
0.2
0.4
0.6
0.8
$\bar{z}$

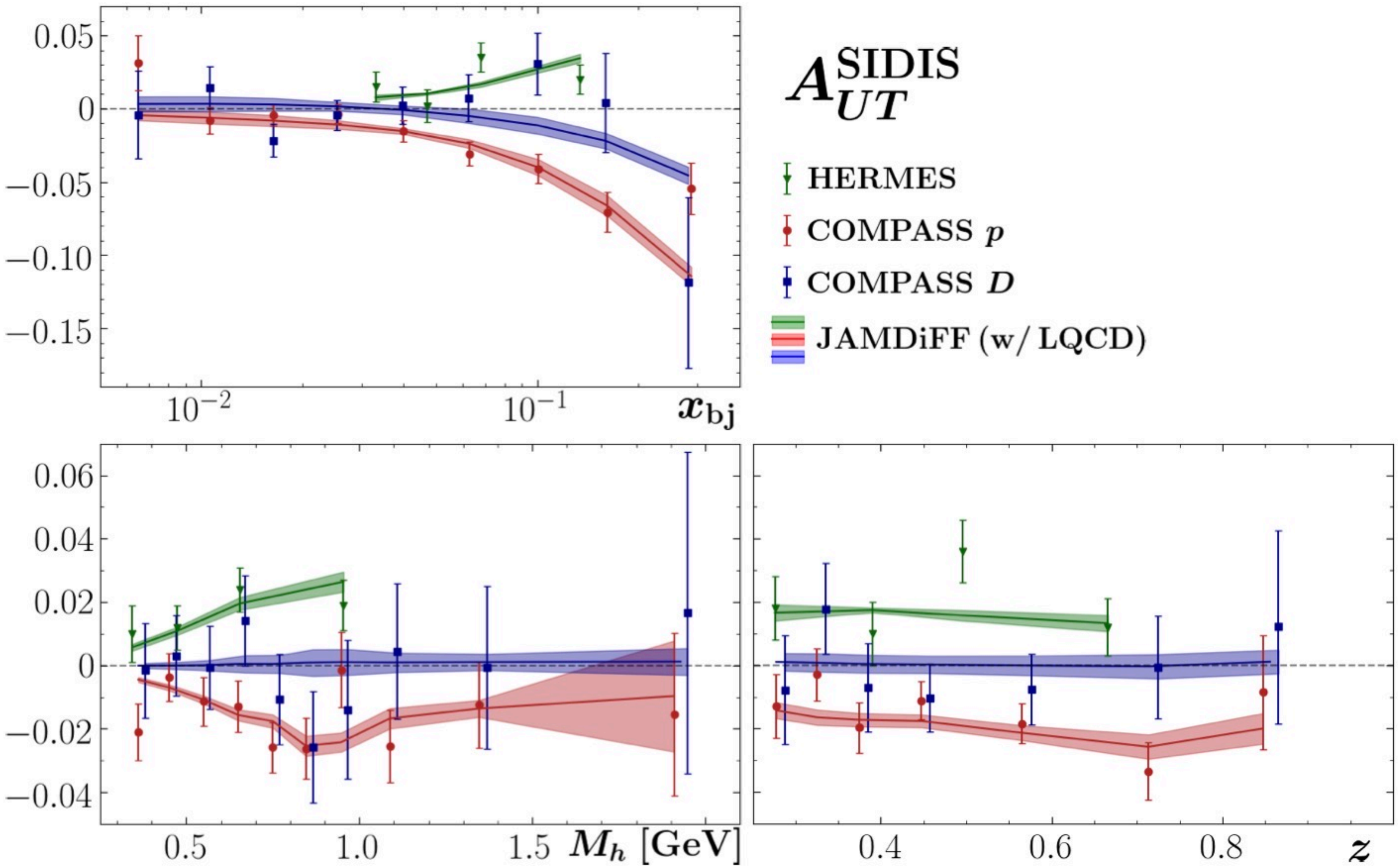
A_{UT}^{SIDIS}
HERMES
COMPASS p
COMPASS D
JAMDiFF (w/ LQCD)
0.05
0
−0.05
−0.10
−0.15
10^{-2}
10^{-1}
x_{bj}
0.06
0.04
0.02
0
−0.02
−0.04
0.5
1.0
1.5
M_h [GeV]
0.4
0.6
0.8
z

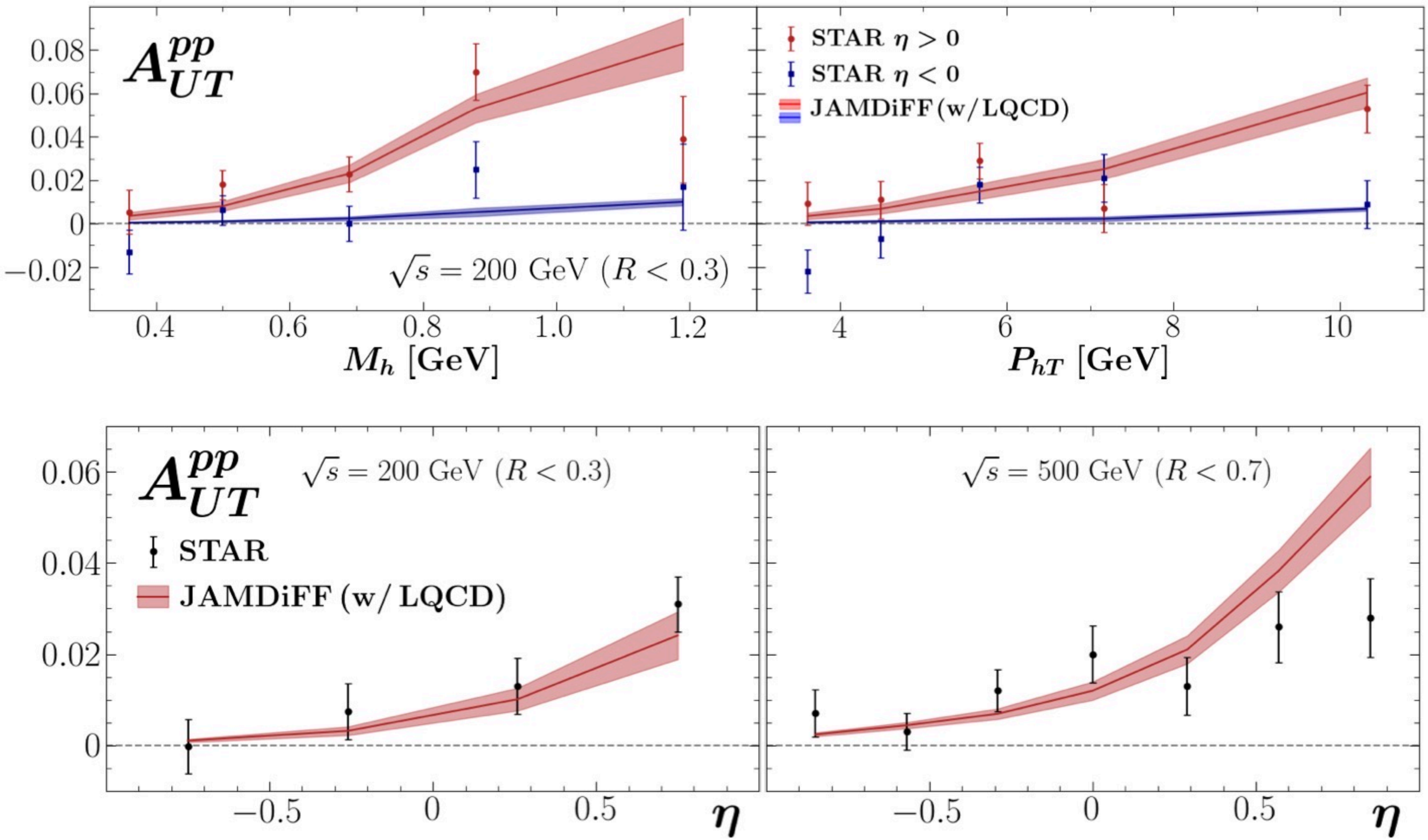
A_{UT}^{pp}
STAR $\eta > 0$
STAR $\eta < 0$
JAMDiFF (w/ LQCD)
$\sqrt{s} = 200$ GeV ($R < 0.3$)
M_h [GeV]
P_{hT} [GeV]
A_{UT}^{pp}
$\sqrt{s} = 200$ GeV ($R < 0.3$)
STAR
JAMDiFF (w/ LQCD)
η
$\sqrt{s} = 500$ GeV ($R < 0.7$)
η

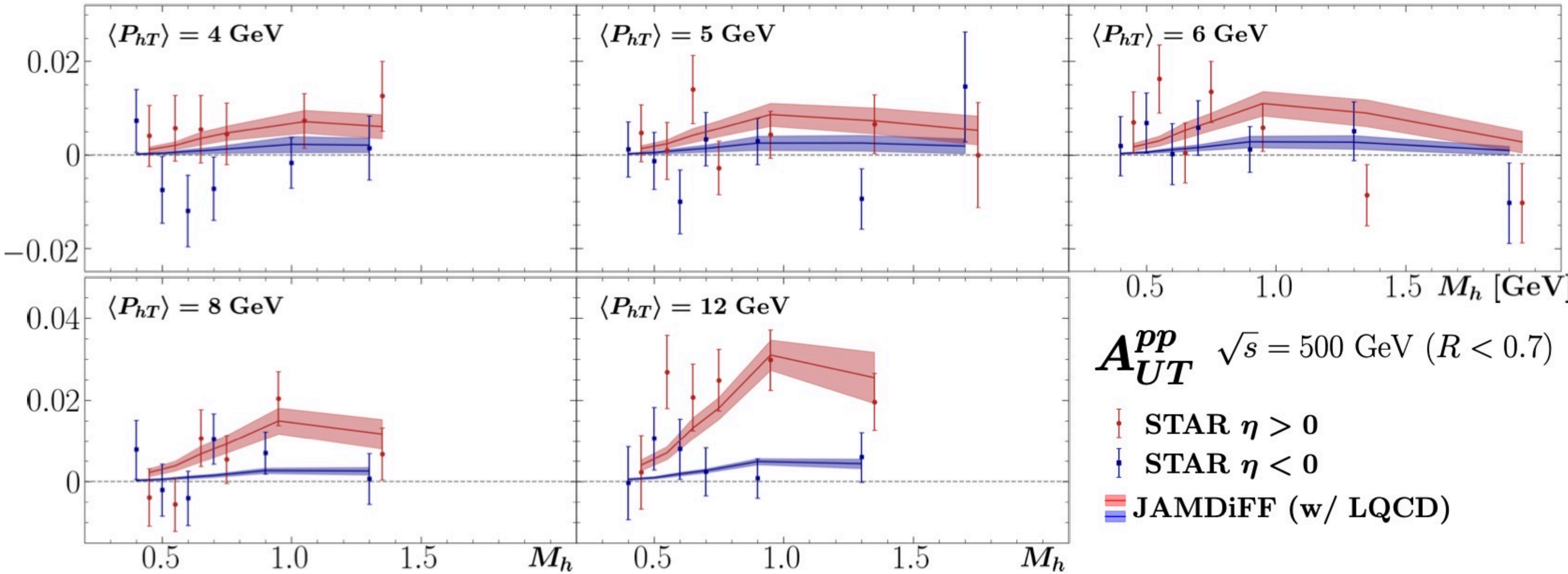
$\langle P_{hT}\rangle = 4$ GeV
$\langle P_{hT}\rangle = 5$ GeV
$\langle P_{hT}\rangle = 6$ GeV
$\langle P_{hT}\rangle = 8$ GeV
$\langle P_{hT}\rangle = 12$ GeV
0.02
0
−0.02
0.04
0.5
1.0
1.5
M_h [GeV]
M_h
A_{UT}^{pp} $\sqrt{s} = 500$ GeV ($R < 0.7$)
STAR $\eta > 0$
STAR $\eta < 0$
JAMDiFF (w/ LQCD)

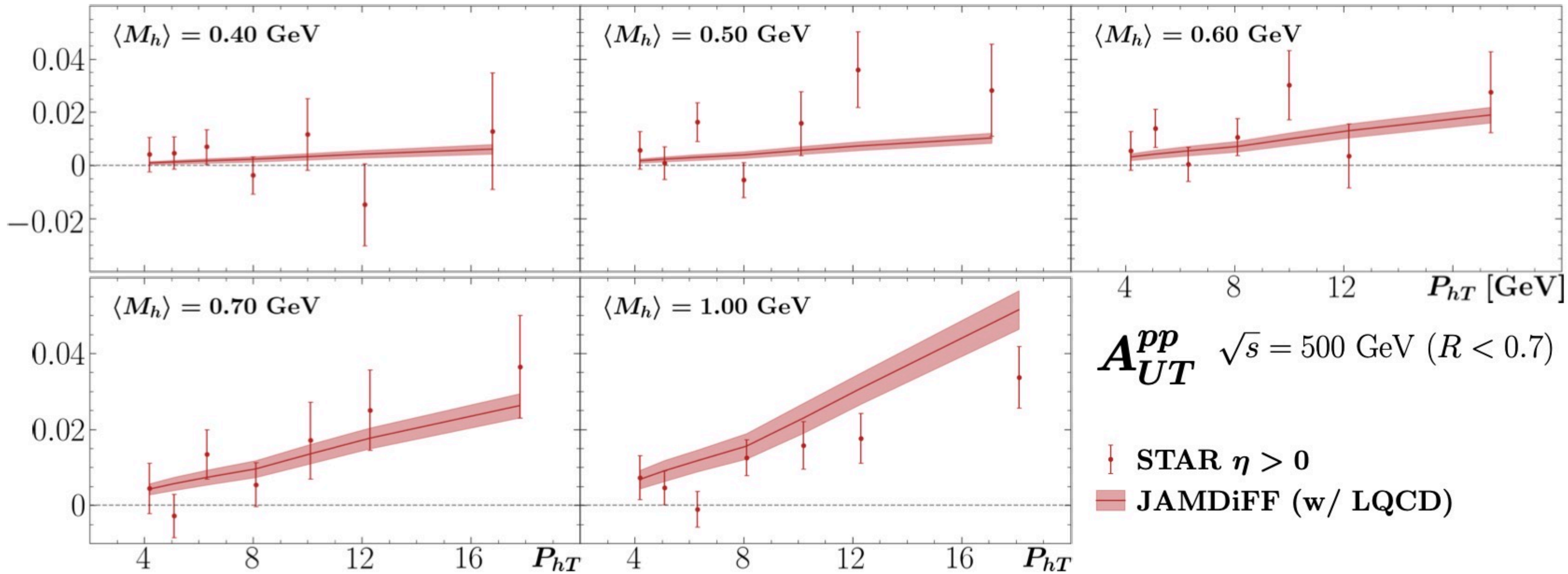
$\langle M_h \rangle = 0.40$ GeV
$\langle M_h \rangle = 0.50$ GeV
$\langle M_h \rangle = 0.60$ GeV
$\langle M_h \rangle = 0.70$ GeV
$\langle M_h \rangle = 1.00$ GeV
0.04
0.02
0
−0.02
4
8
12
16
P_{hT}
P_{hT} [GeV]
A_{UT}^{pp} $\sqrt{s} = 500$ GeV ($R < 0.7$)
STAR $\eta > 0$
JAMDiFF (w/ LQCD)

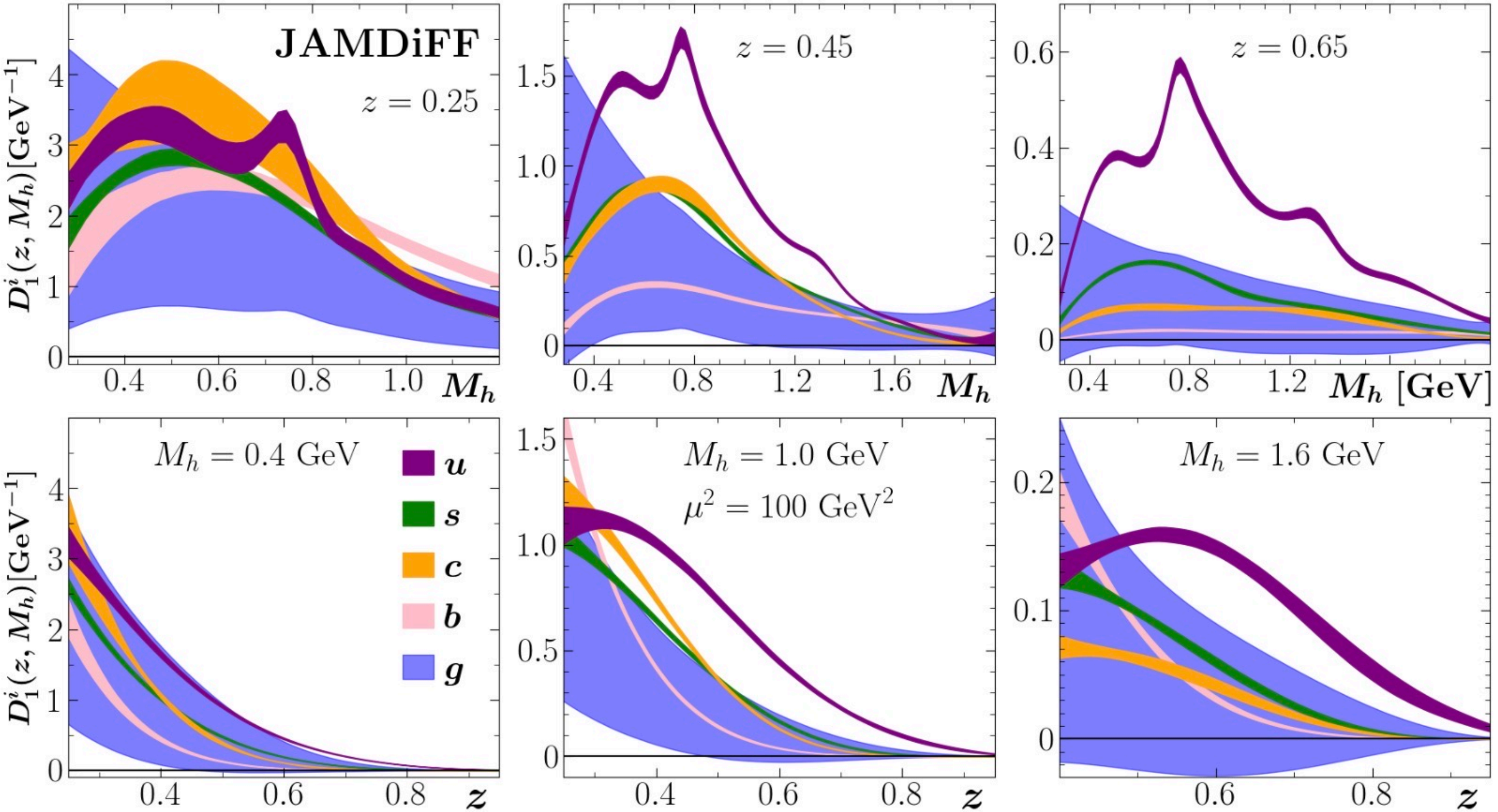
JAMDiFF
z = 0.25
z = 0.45
z = 0.65
$D_1^i(z, M_h)$ [GeV^{-1}]
M_h
M_h [GeV]
M_h = 0.4 GeV
M_h = 1.0 GeV
μ^2 = 100 GeV^2
M_h = 1.6 GeV
u
s
c
b
g
z

- Since $D_1(z,M_h)$ now has a number density interpretation, we can meaningfully calculate expectation values

$$\langle M_h|z\rangle^i = \frac{\int dM_h\, M_h\, D_1^i(z,M_h)}{\int dM_h\, D_1^i(z,M_h)}$$

average value of M_h for a single $\pi^+\pi^-$ pair with a given z formed from the fragmentation of a parton i

$$\langle z|M_h\rangle^i = \frac{\int dz\, z\, D_1^i(z,M_h)}{\int dz\, D_1^i(z,M_h)}$$

average value of z for a single $\pi^+\pi^-$ pair with a given M_h formed from the fragmentation of a parton i

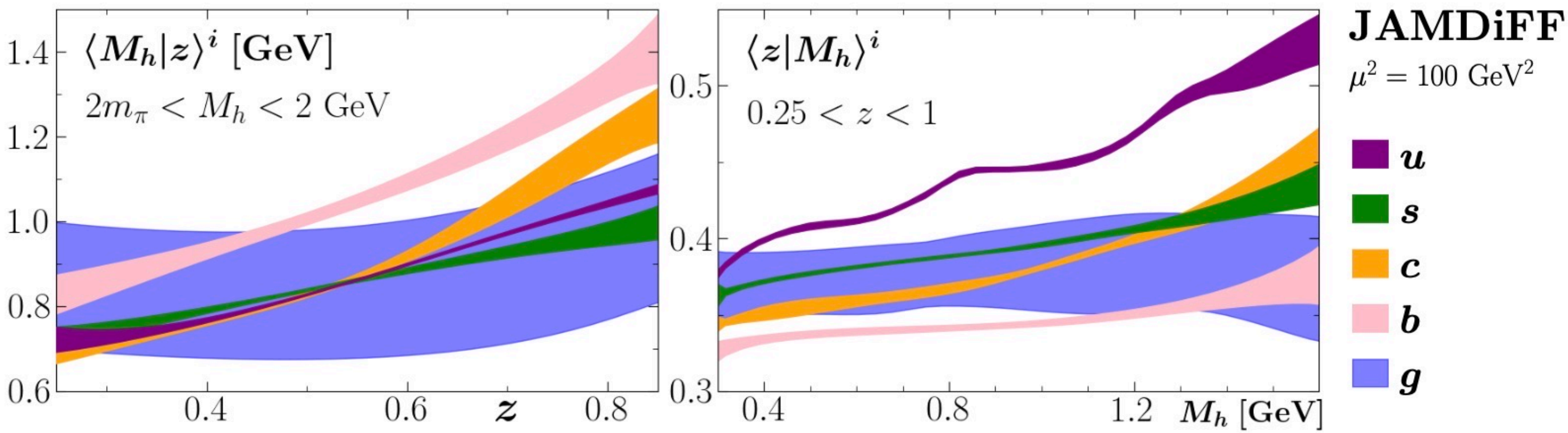

- At smaller z (where more $\pi^+\pi^-$ pairs are produced), we expect on average they will have a smaller mass, in which case the mass of the quark flavor becomes less relevant (b quark is so heavy it separates out even at small z).
- As less $\pi^+\pi^-$ pairs are produced as one nears threshold ($z \rightarrow 1$), then the mass of the quark more directly correlates to the mass of the dihadron.
- For a given M_h, $\pi^+\pi^-$ pairs need to carry smaller z if they arise from the fragmentation of a heavier quark (clear hierarchy is displayed).
- The uncertainty in the gluon DiFF is too large to make any definitive statements about the features of $\pi^+\pi^-$ pairs produced from its fragmentation.

- Response to comment by Rogers and Courtoy - arXiv:2404.02281
  - The potential issue about the violation of the number sum rule equally applies to single-hadron FFs. Nevertheless, the universally accepted number density interpretation of $D_1(z)$ (Collins and Soper (1982)) is not called into question.

- Response to comment by Rogers and Courtoy - arXiv:2404.02281
  - The potential issue about the violation of the number sum rule equally applies to single-hadron FFs. Nevertheless, the universally accepted number density interpretation of $D_1(z)$ (Collins and Soper (1982)) is not called into question.
  - *"Misinterpreting sum rules can have practical numerical consequences for phenomenological analyses"* ... The number sum rule for (single-hadron or dihadron) fragmentation functions (FFs) has never been used to constrain any phenomenological analyses, including those by JAM.

- Response to comment by Rogers and Courtoy - arXiv:2404.02281
  - The potential issue about the violation of the number sum rule equally applies to single-hadron FFs. Nevertheless, the universally accepted number density interpretation of $D_1(z)$ (Collins and Soper (1982)) is not called into question.
  - *"Misinterpreting sum rules can have practical numerical consequences for phenomenological analyses"* … The number sum rule for (single-hadron or dihadron) fragmentation functions (FFs) has never been used to constrain any phenomenological analyses, including those by JAM.
  - "*Note that changes in variables here do not undermine the number density interpretation. If two different variable choices are related by a simple Jacobian J,*

$$\frac{d\hat{N}_h}{d\Phi} = J\frac{d\hat{N}_h}{d\Phi'}$$

then $d\hat{N}_h/d\Phi$ and $d\hat{N}_h/d\Phi'$ *both have equally valid number density interpretations in terms of their respective phase spaces,* $d\Phi$ or $d\Phi'$ *"*

… We agree, as we already made this statement in our paper (see main talk slides), *but it is necessary to first show explicitly that one has defined a function that is a number density* (either for the variable set Φ or Φ')

- Response to comment by Rogers and Courtoy - arXiv:2404.02281 (continued)
  - *"At lowest order in perturbation theory, the Jacobian factor can simply be absorbed into the overall hard factor to maintain consistency with a factorization formula."*

$\ldots\ \tilde{D}_1^{h_1 h_2/q}(z,\zeta,\vec{R}_T^2)$ – different definition of the DiFF that is also *supposed to be a number density in* $(z,\zeta,\vec{R}_T)$

$$\Longrightarrow \frac{d\sigma}{dz\,d\zeta\,d^2\vec{R}_T} = \sum_q (K\,\hat{\sigma}^q)\,\tilde{D}_1^{h_1 h_2/q}(z,\zeta,\vec{R}_T^2)$$

NOT the total partonic cross section for $e^+e^- \to \gamma \to q\bar{q}$

$\Longrightarrow$ $\tilde{D}_1^{h_1 h_2/q}(z,\zeta,\vec{R}_T^2)$ *<u>cannot</u> be a number density in* $(z,\zeta,\vec{R}_T)$